

Single-Crystal Nickel-Cobalt-Manganese Cathode Research

Subjects: [Materials Science](#), [Composites](#)

Contributor: Ruixia Chu , Yujian Zou , Peidong Zhu , Shiwei Tan , Fangyuan Qiu , Wenjun Fu , Fu Niu , Wanyou Huang

The booming electric vehicle industry continues to place higher requirements on power batteries related to economic-cost, power density and safety. The positive electrode materials play an important role in the energy storage performance of the battery. The nickel-rich NCM ($\text{LiNi}_x\text{Co}_y\text{Mn}_z\text{O}_2$ with $x + y + z = 1$) materials have received increasing attention due to their high energy density, which can satisfy the demand of commercial-grade power batteries. Prominently, single-crystal nickel-rich electrodes with a unique micron-scale single-crystal structure possess excellent electrochemical and mechanical performance, even when tested at high rates, high cut-off voltages and high temperatures.

single-crystal

nickel-rich NCM materials

cathode

1. Introduction

Since the economic crisis in 2008, the global energy crisis and environmental pressures are becoming increasingly serious. In order to improve industrial competitiveness, and maintain sustainable economic and social development, the major automobile producing countries (e.g., the United States, Germany, Japan) have adopted the development of electric vehicles as a major strategy ^[1]. At present, the electric vehicle industry is one of the strategic emerging industries pursued by many countries ^{[2][3]}. After decades of development, ever-increasing requirements for energy storage devices have been identified, such as, higher energy density, better safety and longer service life, etc. ^{[4][5]}. However, realization of these goals mainly depends on the cathode material in the power batteries ^{[6][7][8]}.

Ternary layered transition metal oxide, $\text{LiNi}_x\text{Co}_y\text{Mn}_z\text{O}_2$ (NCM, $x + y + z = 1$), was first proposed by J. R. Dahn's group in 2001 ^[9]. According to the report, $\text{Li}[\text{Ni}_x\text{Co}_{1-2x}\text{Mn}_x]\text{O}_2$ with $x = 1/4$ or $3/8$ could be prepared by the "mixed hydroxide" method which combines a two-step calcination process. The obtained samples have a layered α - NaFeO_2 -type structure, and deliver a stable capacity above 150 mAh g^{-1} at the current density of 40 mA g^{-1} in the voltage range of 2.5–4.4 V vs. Li. In particular, the capacity retention behavior of $\text{Li}[\text{Ni}_{3/8}\text{Co}_{1/4}\text{Mn}_{1/4}]\text{O}_2$ was close to that of LiCoO_2 in the same potential window (2.5–4.2 V) and the thermal stability was better. As mentioned above, NCM is based on the hexagonal crystal system of the α - NaFeO_2 -type layered structure, which belongs to the R m space group and can be regarded as a solid solution of three compounds: LiCoO_2 , LiNiO_2 and LiMnO_2 . The layered structure and compositional phase diagram of an NCM cathode are shown as **Figure 1**. the NCM cathode combines the advantages of LiCoO_2 , LiNiO_2 and LiMnO_2 , exhibiting high operating voltage, large energy density

and relatively good cycling performance [10][11][12][13][14][15][16]. In 2021, the Ministry of Industry and Information Technology of the People's Republic of China officially released the "Lithium-ion Battery Industry Specification Conditions (2021)", which states that the energy density of ternary materials-based batteries should not be lower than 210 Wh kg^{-1} , the energy density of battery packs should not less than 150 Wh kg^{-1} , and the specific capacity of ternary materials cathode should not less than 165 Ah kg^{-1} . There has been some research investigating how to improve the stability, safety, and meanwhile reduce the cost of NCM material while ensuring its high energy density [15][17][18].

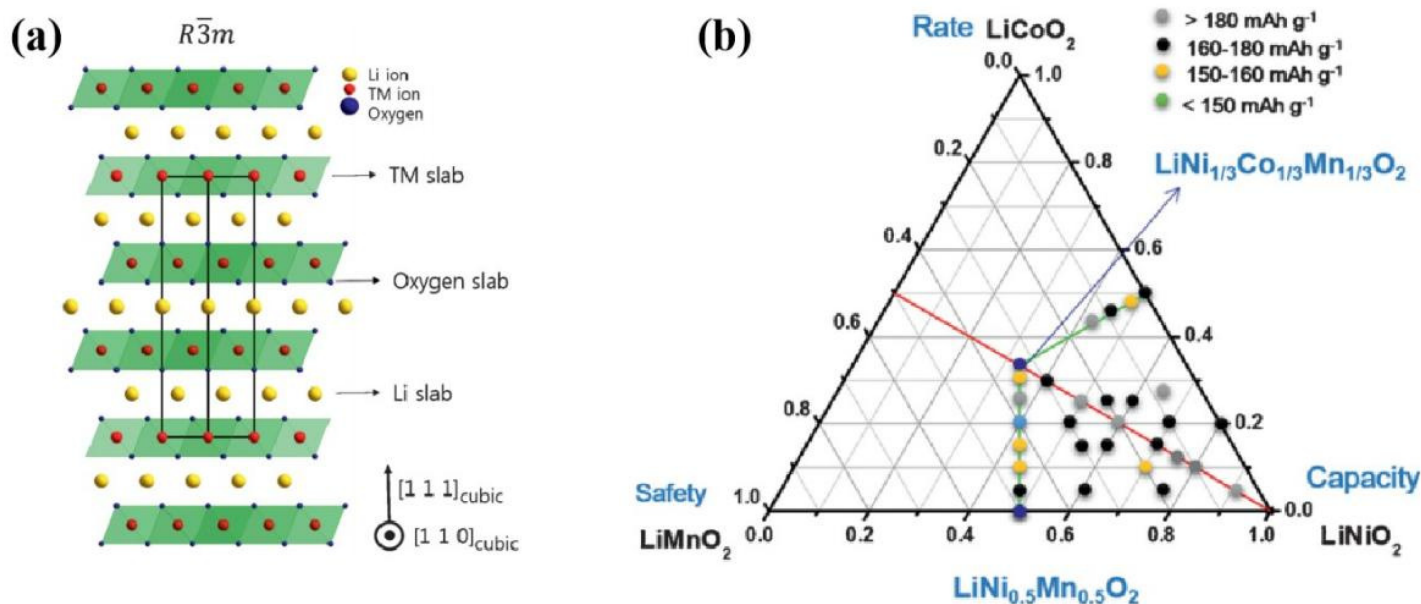


Figure 1. Illustration of the ordered layer structure and phase diagram of NCM materials: (a) the hexagonal crystal system layered structure; (b) NCM composition phase diagram of several typical Ni-Co-Mn ratios, reproduced from Ref. [15], Copyright 2008, The Royal Society of Chemistry.

It is well known that nickel, cobalt and manganese in NCM materials have obvious synergistic effects. Cobalt can stabilize the layered structure, improve electric conductivity, and thus promote the cycle and rate capability for NCM. However, excessive cobalt content leads to more serious economical and environmental problems due to its cost and toxic nature. Nickel can improve the volume energy density of the NCM, while ternary materials with high nickel content lead to cation mixing and cause various problems including capacity loss, structure deterioration and poor thermal stability. Manganese can reduce the costs and improve the safety and structural stability of the NCM. However, a higher manganese content leads to reduced electrochemical activity in the charging/discharging process, and lower specific capacity of the NCM [4][19][20][21][22][23][24][25][26][27][28][29]. For these reasons, numerous scholars have improved the electrochemical properties of NCM by adjusting the elemental ratios of Ni-Co-Mn in order to obtain ternary materials with better performance in all aspects. The relevant NCM materials that have been studied include $\text{LiNi}_{1/3}\text{Co}_{1/3}\text{Mn}_{1/3}\text{O}_2$ (NCM111) [30][31][32][33][34][35], $\text{LiNi}_{0.4}\text{Co}_{0.2}\text{Mn}_{0.4}\text{O}_2$ (NCM424) [30][31][32][33][34], $\text{LiNi}_{0.5}\text{Co}_{0.2}\text{Mn}_{0.3}\text{O}_2$ (NCM523) [36][37][38][39][40][41] and other NCM materials with non-stoichiometry ratios of Ni-Co-Mn elements [42][43][44][45][46][47][48][49][50][51][52], etc. In particular, the nickel-rich NCM materials $\text{LiNi}_{0.6}\text{Co}_{0.2}\text{Mn}_{0.2}\text{O}_2$ (NCM622) [52][53][54][55][56][57][58][59][60][61], $\text{LiNi}_{0.8}\text{Co}_{0.1}\text{Mn}_{0.1}\text{O}_2$ (NCM811) [7][62][63][64][65][66][67][68][69][70][71] and other

NCM with more than 90% nickel content [69][72][73][74][75][76][77][78], even the cobalt-free ternary materials [79][80][81][82][83][84][85][86][87][88][89][90][91], have become increasingly popular active cathode materials because of the higher potential vs. Li, higher energy densities, less toxicity, and lower priced raw materials, which can better meet the needs of electric vehicles. Nevertheless, there still are many remaining challenges in the commercialization of NCM cathodes with high-nickel content ($\text{Ni} \geq 60\%$) including performance deterioration and potential safety concerns. The poor lithium storage and safety of nickel-rich NCM cathodes mainly originate from the following aspects [14][15][16][28][92][93][94][95][96][97][98][99]. (i) During the cycling, heavy Ni^{2+} and Li^+ cation mixing and more vacancies accompanied by oxygen release occur at the stage of the deep delithiation, resulting in irreversible phases transformation from the original layered structure into the spinel-like phase or inactive rock-salt phase, thus leading to poor kinetics, structural stability, thermal stability and cycling performance. (ii) Predomination of the highly oxidized Ni^{4+} ions at the end of charge process leads to a list of issues including the dissolution of transition metal ions, electrolyte decomposition, undesired side interfacial reactions, and the formation of cathode solid electrolyte interfaces (cSEI), which result in low coulombic efficiencies and rapid capacity reduction. (iii) During the lithiation and delithiation process, large lattice volumetric change brings about stress accumulation inside nickel-rich NCM materials, which results in secondary particle microcracks along the grain boundaries, and thus induces further structural degradation and sustained capacity loss.

To address or alleviate the above issues and improve the electrochemical performance of nickel-rich NCM materials, some feasible strategies have been proposed. First, ionic doping is an effective method to stabilize the structure of a nickel-rich NCM electrode. The purpose of doping is to make the dopant ions enter the lattice, replace some of the ions in the raw lattice, stabilize the raw material structure and improve the cycling stability during the charging and discharging process [100][101][102]. In particular, about ten years ago, John B. Goodenough, and Arumugam Manthiram had conducted an in-depth study into the effects of element doping, cation ordering and lithium content on the conductivity and electrochemical characteristics of high-voltage spinel transition metal oxide cathode materials [26][27]. The relationship between the conductivity, phase transformation mechanisms and the content of Mn^{3+} , and the degree of cation ordering were investigated. It was found that Mn^{3+} content and ordering of spinel were not critical to the phase transformation behavior but benefited the high rate capability. Studies of ionic doping in nickel-rich NCM materials include a multitude of dopants such as Mg [102][103], Al [4][102][104][105], Zr [106][107][108], Ti [44][109][110][111], Nb [112][113], Mo [114][115], Cr [116], F [117][118][119][120], B [76][121][122], etc. Proper doping can also boost the cycling performance of the conductivity and lithium ion migration rate of the NCM electrode [15][123]. In addition, the design of the concentration-gradient structured materials can effectively improve the rate and cycling performance [124][125]. Second, surface coating is considered an effective method to improve the capacity retention, rate capability, and thermal stability of an NCM cathode. With the surface coating, the cathode and electrolyte are mechanically separated, and the dissolution of transition metal ions and the interfacial side reaction between cathodes and liquid electrolytes are effectively suppressed, improving the cycling performance of the NCM materials. The surface coating can also reduce the collapse of the material structure during long charging and discharging processes, which is beneficial to the cycling and thermal stability of the NCM materials [15][16][28][92][93][94][95][126][127]. Various coating materials applied on the NCM cathode can be divided into the following categories, such as oxides (SiO_2 [128][129][130], Al_2O_3 [131][132][133][134][135], ZrO_2 [136][137][138][139][140][141], TiO_2 [138][142]

[143][144][145][146], etc.), phosphates (AlPO_4 [147][148], FePO_4 [149][150], $\text{Ni}_3(\text{PO}_4)_2$ [151], CaHPO_4 [152], $\text{Mn}_3(\text{PO}_4)_2$ [153][154], ZrP_2O_7 [155][156], etc.), Li-containing compounds (Li_3PO_4 [157][158][159], Li_2ZrO_3 [160][161][162][163], Li_2TiO_3 [160][164][165], $\text{Li}_{1.5}\text{Al}_{0.5}\text{Ge}_{1.5}(\text{PO}_4)_3$ [166], etc.), electron conducting coatings (graphene or reduced graphene oxide (rGO) [167][168][169][170][171], permeable poly (3,4-ethylenedioxythiophene) (PEDOT) [172][173], polyaniline (PANI) [174][175], polypyrrole (PPy) [176][177], etc.), etc. Combining a concentration gradient and surface coating, the NCM materials with a core-shell structure represent the advantages of the high capacity and high thermal and mechanical stability [178][179]. Third, electrolyte optimization is another effective strategy toward improved performances. As mentioned earlier in the text, the cSEI film reconstruction occurs easily between the solid cathode and organic liquid electrolytes during the cycling, degrading the electrochemical properties of NCM cathodes, especially at high voltages. Different electrolyte additives have been considered to adapt to the high operating voltage of NMC, restrain undesired side reactions and stabilize the surface structure [18][30][46][68][126][180]. With the addition of LiBOB dopamine [181], metal-organic framework (MOF) [182], acetonitrile (AN) [183], vinylene carbonate (VC) [184], fluoroethylene carbonate (FEC) [185] or other tailoring electrolyte additives, the lithium-ion transference number has been effectively increased, the rate capability has been enhanced, and the cycling life has been prolonged [186][187][188]. Typically, the solid-state electrolyte also attracts much attention because of the higher safety and cycling stability compared with combustible organic electrolytes. The solid-state interface engineering strategy is a simple promising method for NCM batteries to meet the ever-increasing requirements of safe power vehicles [189][190][191][192][193][194][195].

Nevertheless, the research about NCM materials summarized above, whether on normal ternary materials or nickel-rich, nickel-ultra-rich or cobalt-free materials, mostly focuses on macro-size polycrystalline secondary spheres composed of nano-size primary grains with random orientations. The continuous growth and expansion of deep-rooted cracking along weak internal grain boundaries still cannot be thoroughly eliminated due to the ever-present anisotropic strain among the randomly oriented primary grains during the charge–discharge process. Although the increasing specific surface area improves the lithium ion conductivity, it aggravates the undesired side reactions between the cathode and electrolyte, increasing the degradation of capacity retention and further reducing the cycling stability. In addition, the internal kinetics of polycrystalline materials are more unstable and the stress distribution is more uneven, especially for nanoscale NCM materials with a higher Ni content or operating voltage (≥ 4.5 V), which makes the materials highly susceptible to structural collapse and capacity decay during prolonged cycling, largely reducing thermal stability and safety [36][67][94][196][197].

2. Synthesis

At present, various synthesis strategies have been developed, including co-precipitation combined with the multi-calcination method (solid-state method) [36][198][199][200][201][202][203][204][205][206][207][208], the molten salt assistant method [209][210][211][212][213][214][215][216][217][218][219][220][221] and the solvothermal method [222][223][224][225]. The main synthesis strategies of single-crystal nickel-rich NCM materials are shown in **Figure 2**.

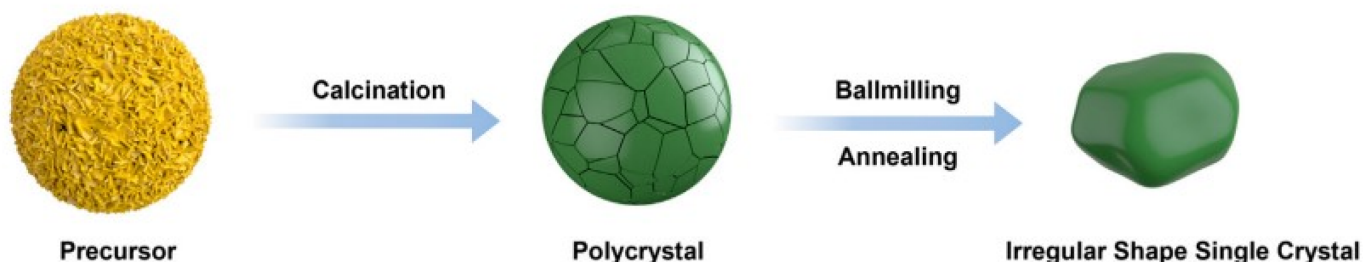
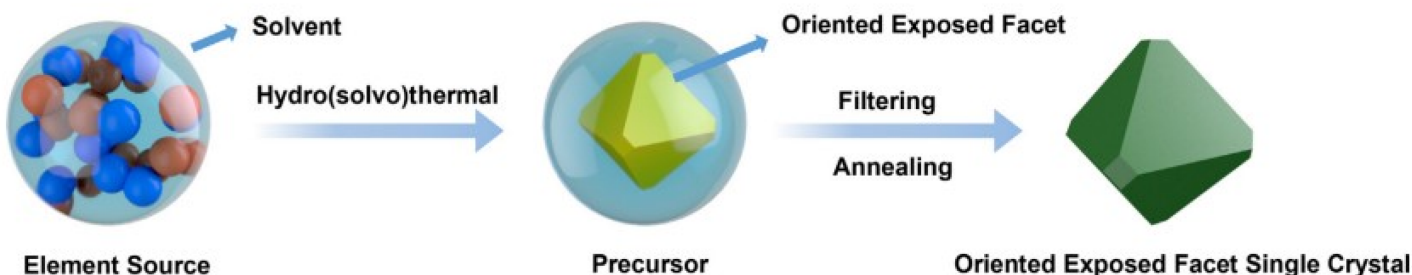
(a) Solid-State Method**(b) Flux Method****(c) Hydrothermal/Solvothermal Method**

Figure 2. A schematic diagrams of the main synthesis strategies for single-crystal nickel-rich NCM materials, reproduced from Ref. [226]. Copyright 2021, Elsevier.

The traditional synthesis strategy of co-precipitation combined with multi-calcination for single-crystal nickel-rich NCM materials usually includes the general co-precipitation method for preparing the precursor and multi-step calcination of the obtained precursor and lithium salt mixture. In the co-precipitation process, a variety of transition metal salts, such as nitrates, sulfates, and hydrochlorides, are commonly used to prepare precursors. In the calcination process, the ratio of the lithium to transition metal (Li/TM) and the temperature are crucial. J. R. Dahn's group introduced co-precipitation (the transition metal sulfates as the source of Ni, Co and Mn) combined with multi-calcination (the as-obtained precursor mixture with Li_2CO_3 were sintered in a box furnace at 930, 950, 970, 990 or 1020 °C for 12 h unless specified, otherwise in air) to synthesize the single-crystal $\text{Li}[\text{Ni}_{0.5}\text{Mn}_{0.3}\text{Co}_{0.2}]\text{O}_2$ material (SC-NCM523) with a grain size of $\sim 2\text{--}5\ \mu\text{m}$. They also discussed the respective effects of the Li/TM ratio, sintering temperature, precursor size and sintering time. The results showed that, the obtained SC-NCM523 displayed good electrochemical performance. Among them, the single-crystal samples prepared at the lowest temperature and minimal Li/TM ratio possessed the highest energy density [198]. At the same time, the group made a comparative study of the synthesized SC-NCM523, the conventional polycrystalline NCM523 and polycrystalline

Al₂O₃-coated NCM523 by assembling pouch cells and coin cells with graphite as the negative electrode via multiple advanced means. The long-term cycling tests showed that cells with SC-NCM523 exhibited much better capacity retention but slightly lower specific capacity than that of the cells with polycrystalline cathodes when tested to an upper cut-off potential of 4.4 V [36]. Xinming Fan's group exploited a one-step calcination method, which is a more simplified and lower cost process than the traditional multi-calcination method. As summarized in **Figure 3**, a single-crystalline LiNi_{0.6}Co_{0.1}Mn_{0.3}O₂ (NCM613) was synthesized with an excess lithium source (an Li/M ratio of 1.08:1), under 930 °C in air. According to the morphology characterization and electrochemical test results, the as-prepared NCM613 had a suitable micron-size particle with a robust and stable primary particle grains. The NCM613/graphite full cell delivered a capacity retention of 73.9% after 900 cycles at 1 C at the working temperature of 45 °C with the cut-off voltage of 4.2 V [227]. In-depth studies indicated that the energy density, electrochemical performance and thermal stability were significantly improved at 55 °C under a high charging voltage of 4.4 V. The single-crystal NCM622 material (SC-NCM622) obtained with same method showed a much more robust particle structure without crack formation during cycling. The SC-NCM622/graphite pouch cells with a cathode areal capacity of 6 mAh cm⁻² exhibited an excellent capacity retention of 83% after 3000 cycles, demonstrating the effectiveness of a single-crystal approach in mitigating degradation in the lithium-ion battery cathode [228].

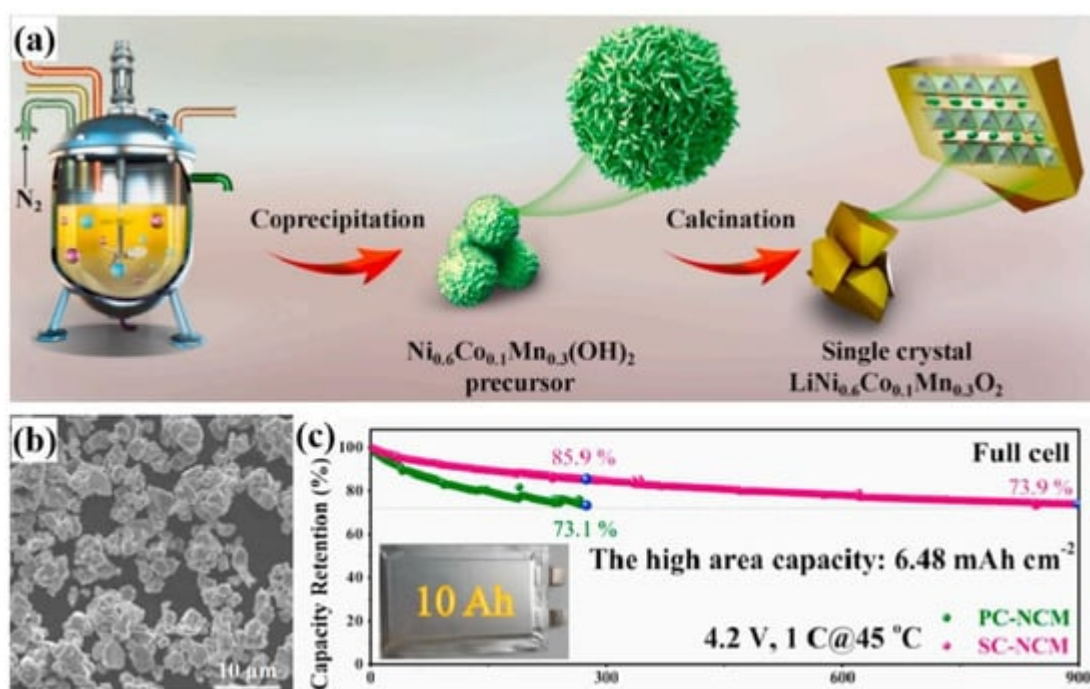


Figure 3. Research content reproduced from Ref. [227] of Xinming Fan's group: (a) schematic diagram of preparation process and (b) SEM image for single-crystal NCM613, (c) the cycling performance of NCM613/graphite full cell, Copyright 2021, Elsevier.

However, the calcination temperature required for the preparation of single-crystal nickel-rich NCM materials is too high, basically above 900 °C, a temperature which would destroy the layered structure. To overcome this problem, Yang-Kook Sun's group developed a calcination method under an oxygen atmosphere, during which the sintering

temperature was 50 °C lower than the optimal calcination temperature. The reduction of annealing temperature in this work was realized by Ce doping, which is thought to promote the formation of single-crystals. As a result, a single-crystal Ce-doped $\text{Li}[\text{Ni}_{0.9}\text{Co}_{0.05}\text{Mn}_{0.05}]\text{O}_2$ (SC NCM90) material with ultra-high nickel content was obtained at 800 °C. The material delivered excellent electrochemical performance in terms of a high initial discharge specific capacity of 199.7 mAh g⁻¹ at 0.1 C, high capacity retention (80.5% of the initial capacity after 100 cycles at 0.5 C) and better cycling stability [229]. Yet the single-crystal pristine $\text{Li}[\text{Ni}_{0.9}\text{Co}_{0.05}\text{Mn}_{0.05}]\text{O}_2$ (Pri-NCM90) synthesized at 850 °C demonstrated comparatively inferior capacity retention and thermal stability. Moreover, the group conducted an in-depth analysis on the structural instability of charged single-crystal $\text{Li}[\text{Ni}_{0.9}\text{Co}_{0.05}\text{Mn}_{0.05}]\text{O}_2$ (SC-NCM90) and $\text{Li}[\text{Ni}_{0.7}\text{Co}_{0.15}\text{Mn}_{0.15}]\text{O}_2$ (SC-NCM70) without any dopants. The results showed that there was no irreversible structural damage in SC-NCM70 when charged to 4.3 V, while the significant intra-particle submicroscopic cracks appeared at the multiple phase boundaries of charged SC-NCM90. The analysis emphasized that the internal strain generated by the phase transition is aggravated by inhomogeneous distribution of Li, causing the fundamental structural instability [208]. In addition, J. R. Dahn's group further prepared Co-free Ni-rich single-crystal cathode materials based on a multi-step calcination method during which a preheated process was introduced [230][231][232]. The relevant reports analyzed the effects of heating temperature, Li/TM ratio and lower temperature steps on the properties of the composite materials.

The molten salt assistant method is another commonly used strategy to synthesize high-quality nickel-rich NCM materials at lower temperatures. Hyun-Soo Kim and his co-workers prepared a single-crystal NCM material with ultra-high nickel content by a flux method with LiCl-NaCl as a molten salt [220], which was denoted as $\text{LiNi}_{0.91}\text{Co}_{0.06}\text{Mn}_{0.03}\text{O}_2$ (SNCM91). When used as the cathode for a lithium battery, SNCM91 displayed favorable morphology retention during cycling and a high initial discharge capacity of 203.8 mAh g⁻¹ at 0.1 C in the voltage range of 3.0–4.3 V, demonstrating excellent initial specific capacity as a nickel-ultra-rich NCM material. Similarly, Yuzong Gu's group synthesized nickel-ultra-rich single-crystalline $\text{LiNi}_{0.92}\text{Co}_{0.06}\text{Mn}_{0.02}\text{O}_2$ powder (SC-780) by a novel LiOH-LiNO₃-H₃BO₃ ternary molten-salt method with a calcination temperature of 780 °C for 20 h under an oxygen atmosphere [213]. When tested as the cathode in a pouch-type full cell at 45 °C, the as-obtained SC-780 exhibited excellent long-term cycling performance in terms of a superior initial discharge capacity of 214.8 mAh g⁻¹ at 0.5 C in the voltage range of 2.7–4.2 V, and a high-capacity retention of 86.3% over 300 cycles. The flux of H₃BO₃ can regulate crystal growth to improve the particles' uniformity and monodispersity. Meanwhile, a small amount of boron doping with stronger B-O covalent bonds may promote the structural stability and expand the layered distance, ensuring the enhanced electrochemical kinetics.

The advantages of melting characteristics and excellent flowability for molten salt assistants provokes much attention and thinking. For example, Wuwei Yan and his co-workers prepared single-crystal $\text{LiNi}_{0.92}\text{Co}_{0.06}\text{Mn}_{0.01}\text{Al}_{0.01}\text{O}_2$ (NCMA) cathode materials with ammonium metatungstate and ammonium molybdate as the co-doping fluxing agents and doping materials [218]. Due to the co-doping fluxing strategy, the as-prepared NCMA had a smaller particle size, less cationic mixing, a more stable phase structure and less internal resistance, displaying superior electrochemical performance. The optimal NCMA contained 1000 ppm W and 1000 ppm Mo (NCMA-B), displaying a higher initial discharge capacity of 221.4 mAh g⁻¹ at 0.1 C in the voltage range of 3.0–4.3 V, and the corresponding capacity retention after 100 cycles at 25 °C and 45 °C was 95.7% and 94.9%,

respectively. Notably, Xiaobo Ji's group successfully designed and prepared a single-crystalline Co-free Ni-rich $\text{LiNi}_{0.95}\text{Mn}_{0.05}\text{O}_2$ (SC-NM95) layered cathode without any cracks, as shown in **Figure 4a**, during which the LiOH and LiNO_3 were mixed homogeneously as the molten salt system and lithium source [215]. When tested at 0.1 C with an operating voltage of 2.7–4.3 V, the obtained SC-NM95 cathode achieved a high initial discharge capacity of 218.2 mAh g^{-1} , a high energy density of 837.3 Wh kg^{-1} , and an outstanding capacity retention (84.4%) after 200 cycles at 1 C. Even in the extended voltage range of 2.7–4.5 V, SC-NM95 showed a superior initial capacity of 230.1 mAh g^{-1} with a Coulomb Efficiency of 86.48%. A capacity retention of 81% was achieved after 100 cycles, indicating the reinforced electrochemical reversibility and cycling stability at a high cut-off voltage (**Figure 4b–d**).

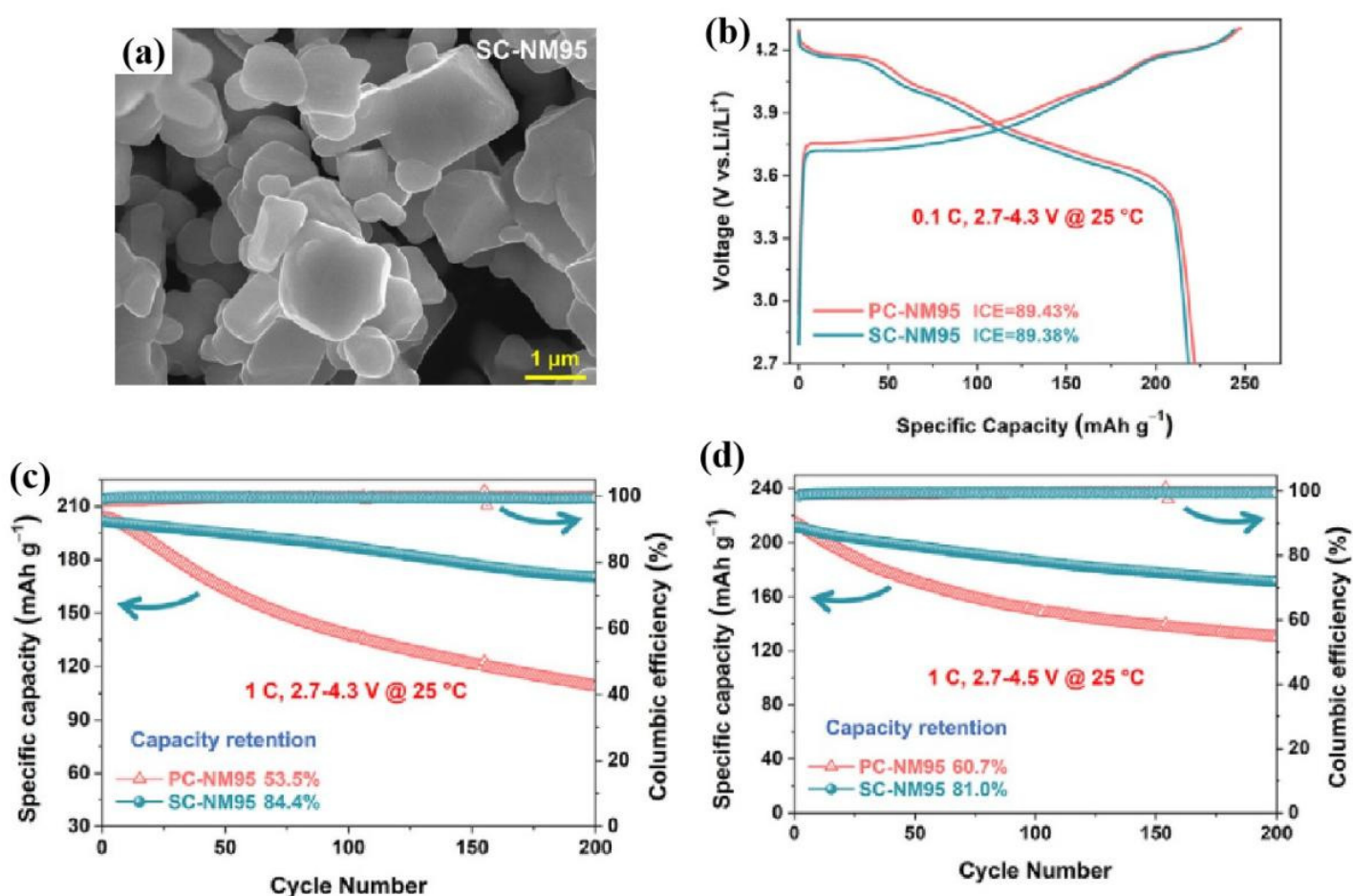


Figure 4. Research content reproduced from Ref. [215]: (a) SEM image of fresh SC-NM95 materials; (b) the first discharge/charge curves, and the cycling performance at difficult cut-off voltage of (c) 4.3 V and (d) 4.5 V of comparison between SC-NM95 and PC-NM95 materials, Copyright 2022, Elsevier.

Additionally, in order to alleviate the environmental impact of waste lithium-ion batteries and the rising cost of cathode materials, the molten salt assistant methods are also commonly used to extract transition metal elements from spent polycrystalline layered cathode materials [216][217]. For instance, Weixin Zhang's group developed a simple and effective strategy to recycle spent polycrystalline ternary cathode materials into single-crystal cathodes which is based on an alkaline LiOH-LiNO_3 molten salt [216]. The Li-based molten salt system repaired the lithium defects and the damaged structures generated during repeated lithium and (de)lithiation process. The as-obtained

plate-like single-crystal NCM622 with exposed (010) planes delivered a high capacity of 155.1 mAh g⁻¹ at 1 C in the operating voltage range of 2.8–4.3 V and a superior long cycling stability of about 94.3% capacity retention, even after 240 cycles. Significantly, the recycling method can be expanded to other waste Ni-Co-Mn ternary cathode materials or their mixtures for producing high-performance single-crystal cathode materials to utilize the large amounts of waste lithium-ion batteries, thus facilitating green and sustainable development.

The solvothermal method, including hydrothermal method, is a synthesis method for the reaction of the original mixture in a closed system, using organic matter or a non-aqueous solvent (the solvent for the hydrothermal reaction is water) under a certain high-temperature and high-pressure environment. In this method, the phase formation, particle size and morphology of the prepared samples can be well controlled, resulting in better dispersion of the product. The reaction process is greatly affected by solvent type, reactant ion concentration and reaction temperature and time. The solvothermal method is commonly used to prepare micro or nano materials with specific morphology. For NCM materials, single-crystal nickel-rich NCM materials with a specific crystal plane orientation can be obtained by the solvothermal method. Jianguo Duan's group prepared a hexagonal morphology Ni_{0.8}Co_{0.1}Mn_{0.1}(OH)₂ precursor with the preferred orientation of (001) lattice plane [222]. After the sintering process at a lower reaction temperature (780 °C) and lower excess lithium/transition metal ratio (1.03:1), the highly-crystalline micrometer-sized Ni-rich single-crystal LiNi_{0.8}Co_{0.1}Mn_{0.1}O₂ (SC-NCM) with the retained precursor hexagonal morphology was obtained (the preparation process and corresponding SEM image are illustrated in **Figure 5a,b**). All the primary particles of SC-NCM displayed smooth surfaces with legible grain boundaries, a lower specific surface area, stable crystal plane exposure, unimpeded Li⁺ transport structure, larger C-axis, and lower sulfur impurities. The electrochemical test results conducted in a CR2025 coin-type cell showed an initial capacity of 186.2 mAh g⁻¹ at 1 C during 2.8–4.3 V and a capacity retention of ~93.4% after 100 cycles (**Figure 5c**). Even when the rate was increased to 10 C, the SC-NCM cathode achieved a capacity of 130.4 mAh g⁻¹, representing an excellent rate performance (**Figure 5d**). Youxiang Zhang's group also prepared single-crystal LiNi_{0.8}Co_{0.1}Mn_{0.1}O₂ by the simple solvothermal method combined with a lower calcination temperature. However, the obtained sample displayed a different rod-like morphology [223]. When the excess lithium content was 50%, the LiNi_{0.8}Co_{0.1}Mn_{0.1}O₂ (NCM811) material showed uniform mono-dispersed rod particles with a micrometer-scale and good crystallinity and showed an excellent discharge capacity and cycling stability (a high initial discharge capacity of 226.9 mAh g⁻¹ with a Coulombic Efficiency of 91.2% at 0.1 C in the voltage range of 2.8–4.3 V). When the current density increased to ten times of the original, the discharge capacity could still reach 178.1 mAh g⁻¹ with a capacity retention of 95.1% after 100 cycles. The excellent high-rate cycling performance was mainly attributed to the lower specific area, weaker cation mixing, and uniform particle distribution.

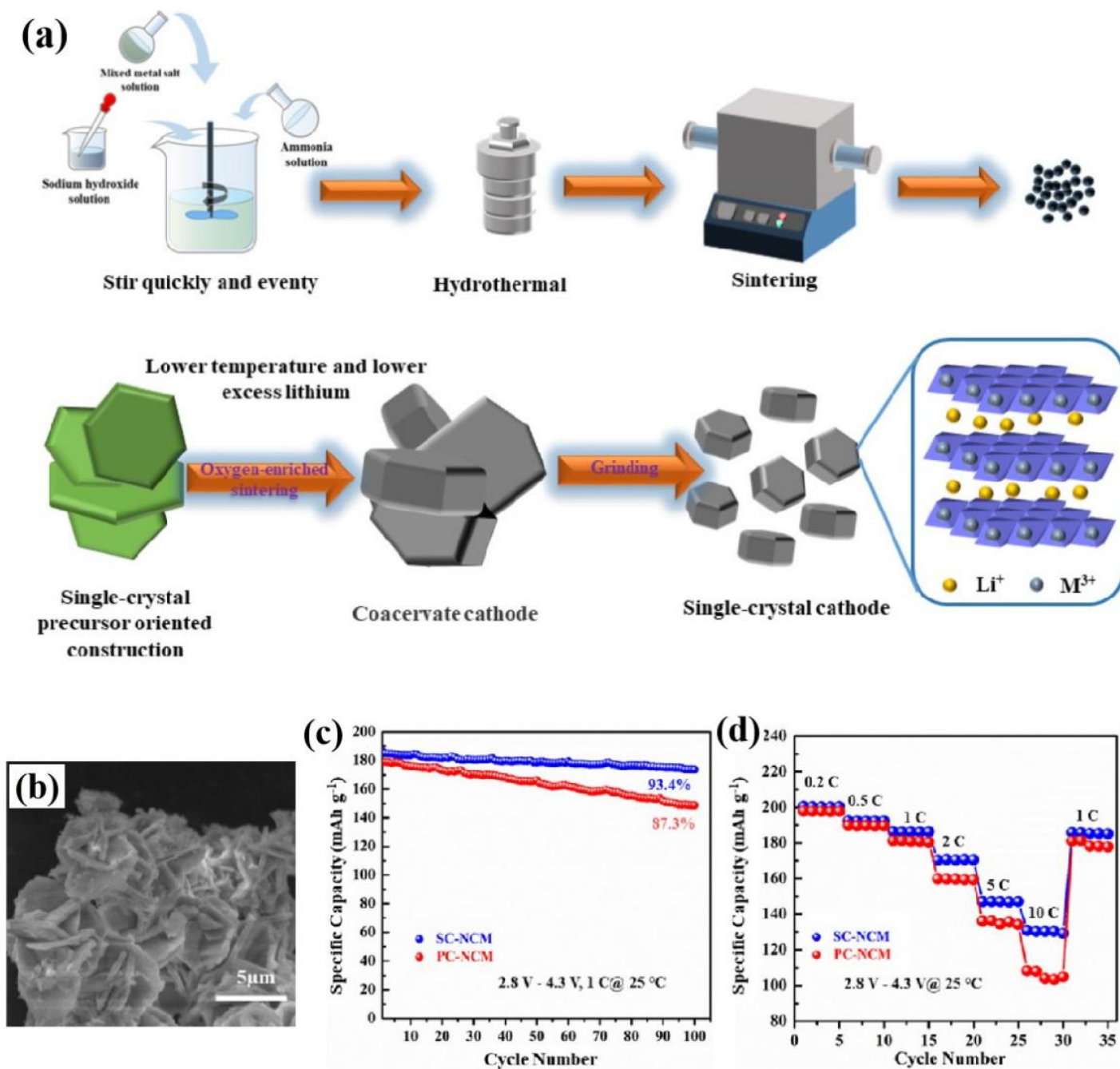


Figure 5. Research content reproduced from Ref. [222]. (a) The schematic diagram for the preparation process and (b) SEM image for SC-NCM. The comparison of (c) cycling performance and (d) rate capability between SC-NCM and PC-NCM, Copyright 2022, American Chemical Society.

As is well-known, the pH value is another important parameter influencing the solvothermal method, which is critical to the lattice structure and morphology of products. Ke Du and his co-workers prepared single-crystalline $\text{LiNi}_{0.6}\text{Co}_{0.2}\text{Mn}_{0.2}\text{O}_2$ (SC-NCM) with hexagonal slabs by the hydrothermal method [224]. In this hydrothermal process, $\text{NH}_3\cdot\text{H}_2\text{O}$ was used as the precipitant, and the value of pH was adjusted to 9.6. The morphology and electrochemical characterization demonstrated that SC-NCM displayed micro-sized particles with a highly-ordered layer structure, and had excellent capacity retentions of 93.2% and 89.6% at 1 C after 100 cycles at the cut-off

potentials of 4.3 V and 4.5 V, respectively. The lower cation mixing and fine grain size of the SC-NCM primary particle inhibited structural collapse and promoted lithium ion transport, thus elevating the rate capability.

The electrochemical properties of single-crystal nickel-rich NCM materials synthesized via different strategies are reported in **Table 1**.

Table 1. Electrochemical properties of single-crystal nickel-rich NCM materials synthesized via different strategies. (CR = Capacity Retention).

Material Components	Synthesis Methods	Electrochemical Performance	Ref.
$\text{LiNi}_{0.6}\text{Co}_{0.1}\text{Mn}_{0.3}\text{O}_2$ (SC-NCM613)	One-step calcination method	CR of 73.9% after 900 cycles at 1 C, 45 °C, 2.75–4.2 V, pouch full cell	[227]
$\text{LiNi}_{0.6}\text{Co}_{0.2}\text{Mn}_{0.2}\text{O}_2$ (SC-NCM622)	One-step calcination method	CR of 82.6% after 3000 cycles at 1 C, 25 °C, 3.0–4.2 V, pouch full cell	[228]
Ce-doped $\text{Li}[\text{Ni}_{0.9}\text{Co}_{0.05}\text{Mn}_{0.05}]\text{O}_2$ (SC-Ce-NCM90)	One-step calcination method with lower temperature	CR of 80.5% after 100 cycles at 0.5 C, 30 °C, 2.7–4.3 V, half cell	[229]
$\text{Li}[\text{Ni}_{0.7}\text{Co}_{0.15}\text{Mn}_{0.15}]\text{O}_2$ (SC-NCM70)	Calcination method	CR of 91% after 100 cycles at 0.5 C, 30 °C, 2.7–4.3 V, half cell	[208]
$\text{LiNi}_{0.91}\text{Co}_{0.06}\text{Mn}_{0.03}\text{O}_2$ (SNCM91)	Molten salt assistant method	initial discharge capacity of 203.8 mAh g^{-1} at 0.1 C, 3.0–4.3 V, half cell	[220]
$\text{LiNi}_{0.92}\text{Co}_{0.06}\text{Mn}_{0.02}\text{O}_2$	Molten salt assistant method	CR of 86.3% after 300 cycles at 0.5 C, 25 °C, 2.7–4.2 V, pouch full cell	[213]
$\text{LiNi}_{0.92}\text{Co}_{0.06}\text{Mn}_{0.01}\text{Al}_{0.01}\text{O}_2$ (NCMA)	Solid-phase sintering method	221.4 mAh g^{-1} at 0.1 C, 3.0–4.3 V, CR of 94.9% after 100 cycles at 45 °C, half cell	[218]
$\text{LiNi}_{0.95}\text{Mn}_{0.05}\text{O}_2$ (SC-NM95)	Molten salt assistant method	CR of 81% after 200 cycles at 1 C, 25 °C, 2.7–4.5 V, half cell	[215]
$\text{LiNi}_{0.6}\text{Co}_{0.2}\text{Mn}_{0.2}\text{O}_2$ (SC-NCM622)	Molten salt assistant method	155.1 mAh g^{-1} at 1 C, CR of 94.3% after 240 cycles at 1 C, 25 °C, 2.8–4.3 V, half cell	[216]
$\text{LiNi}_{0.8}\text{Co}_{0.1}\text{Mn}_{0.1}\text{O}_2$ (SC-NCM811)	Hydrothermal method	186.2 mAh g^{-1} at 1 C, CR of 93.4% after 100 cycles at 1 C, 25 °C, 2.8–4.3 V, half cell	[222]
$\text{LiNi}_{0.8}\text{Co}_{0.1}\text{Mn}_{0.1}\text{O}_2$ (SC-NCM811)	Solvothermal method	226.9 mAh g^{-1} at 0.1 C, CR of 91.2% after 100 cycles at 1 C, 25 °C, 2.8–4.3 V, half cell	[223]

In addition to the methods summarized above, the synthesis strategies of ion anchoring [233], sol-gel [234], etching [235], and other advanced methods [236][237][238][239] are usually employed to produce single-crystal nickel-rich NCM

Material Components	Synthesis Methods	Electrochemical Performance	Ref.
$\text{LiNi}_{0.6}\text{Co}_{0.2}\text{Mn}_{0.2}\text{O}_2$ (SC-NCM622)	Hydrothermal method	184.2 mAh g ⁻¹ at 0.1 C, CR of 89.6% after 100 cycles at 1 C, 2.8–4.5 V, half cell	[224]

References

- Armand, M.; Tarascon, J.M. Building better batteries: Researchers must find a sustainable way of providing the power our modern lifestyles demand. *Nature* 2008, 451, 652–657.
- Manthiram, A.; Song, B.; Li, W. A perspective on nickel-rich layered oxide cathodes for lithium-ion batteries. *Energy Storage Mater.* 2017, 6, 125–139.
- Tarascon, J.M.; Armand, M. Issues and challenges facing rechargeable lithium batteries. *Nature* 2001, 414, 359–367.
- Whittingham, M.S. Lithium batteries and cathode materials. *Chem. Rev.* 2004, 104, 4271–4301.
- Andre, D.; Kim, S.J.; Lamp, P.; Lux, S.F.; Maglia, F.; Paschos, O.; Stiaszny, B. Future generations of cathode materials: An automotive industry perspective. *J. Mater. Chem. A* 2015, 3, 6709–6732.
- Zaghib, K.; Mauger, A.; Groult, H.; Goodenough, J.B.; Julien, C.M. Advanced electrodes for high power Li-ion batteries. *Materials* 2013, 6, 1028–1049.
- Li, W.; Erickson, E.M.; Manthiram, A. High-nickel layered oxide cathodes for lithium-based automotive batteries. *Nat. Energy* 2020, 5, 26–34.
- Akhilash, M.; Salini, P.S.; John, B.; Mercy, T.D. A journey through layered cathode materials for lithium ion cells—From lithium cobalt oxide to lithium-rich transition metal oxides. *J. Alloys Compd.* 2021, 869, 159239.
- Lu, Z.; MacNeil, D.D.; Dahn, J.R. Layered LiO₂ cathode materials for lithium-ion batteries. *Electrochem. Solid-State Lett.* 2001, 4, 200–203.
- Ohzuku, T.; Makimura, Y. Layered Lithium Insertion Material of LiCo_{1/3}Ni_{1/3}Mn_{1/3}O₂ for Lithium-Ion Batteries. *Chem. Lett.* 2001, 30, 642–643.
- Hwang, B.J.; Tsai, Y.W.; Carlier, D.; Ceder, G. A Combined computational/experimental study on LiNi_{1/3}Co_{1/3}Mn_{1/3}O₂. *Chem. Mater.* 2003, 15, 3676–3682.
- Radin, M.D.; Hy, S.; Sina, M.; Fang, C.; Liu, H.; Vinckeviciute, J.; Zhang, M.; Whittingham, M.S.; Meng, Y.S.; Van der Ven, A. Narrowing the gap between theoretical and practical capacities in Li-ion layered oxide cathode materials. *Adv. Energy Mater.* 2017, 7, 1602888.
- Goodenough, J.B.; Kim, Y. Challenges for Rechargeable Li Batteries. *Chem. Mater.* 2009, 22, 587–603.
- Chakraborty, A.; Kunnikuruvaan, S.; Dixit, M.; Major, D.T. Review of computational studies of NCM cathode materials for Li-ion batteries. *Isr. J. Chem.* 2020, 60, 850–862.

15. Liu, W.; Oh, P.; Liu, X.; Lee, M.J.; Cho, W.; Chae, S.; Kim, Y.; Cho, J. Nickel-rich layered lithium transition-metal oxide for high-energy lithium-ion batteries. *Angew. Chem. Int. Ed.* 2015, 54, 4440–4457.
16. Jung, C.H.; Shim, H.; Eum, D.; Hong, S.H. Challenges and recent progress in $\text{LiNi}_x\text{Co}_y\text{Mn}_{1-x-y}\text{O}_2$ (NCM) cathodes for lithium ion batteries. *J. Korean Ceram. Soc.* 2020, 58, 1–27.
17. Li, W.; Dolocan, A.; Oh, P.; Celio, H.; Park, S.; Cho, J.; Manthiram, A. Dynamic behaviour of interphases and its implication on high-energy-density cathode materials in lithium-ion batteries. *Nat. Commun.* 2017, 8, 14589.
18. Maleki Kheimeh Sari, H.; Li, X. Controllable cathode–electrolyte interface of LiO_2 for lithium ion batteries: A review. *Adv. Energy Mater.* 2019, 9, 1901597.
19. Lim, B.B.; Yoon, S.J.; Park, K.J.; Yoon, C.S.; Kim, S.J.; Lee, J.J.; Sun, Y.K. Advanced concentration gradient cathode material with two-slope for high-energy and safe lithium batteries. *Adv. Funct. Mater.* 2015, 25, 4673–4680.
20. Koyama, Y.; Arai, H.; Tanaka, I.; Uchimoto, Y.; Ogumi, Z. Defect chemistry in layered LiMO_2 (M = Co, Ni, Mn, and $\text{Li}_{1/3}\text{Mn}_{2/3}$) by first-principles calculations. *Chem. Mater.* 2012, 24, 3886–3894.
21. Zheng, J.; Liu, T.; Hu, Z.; Wei, Y.; Song, X.; Ren, Y.; Wang, W.; Rao, M.; Lin, Y.; Chen, Z.; et al. Tuning of thermal stability in layered $\text{Li}(\text{Ni}_x\text{Mn}_y\text{Co}_z)\text{O}_2$. *J. Am. Chem. Soc.* 2016, 138, 13326–13334.
22. Kim, J. Synthesis and electrochemical behavior of LiO_2 cathode materials. *Solid State Ionics* 2003, 164, 43–49.
23. Kang, K.; Ceder, G. Factors that affect Li mobility in layered lithium transition metal oxides. *Phys. Rev. B* 2006, 74, 094105.
24. Huang, Z.; Gao, J.; He, X.; Li, J.; Jiang, C. Well-ordered spherical $\text{LiNi}_x\text{Co}_{(1-2x)}\text{Mn}_x\text{O}_2$ cathode materials synthesized from cobalt concentration-gradient precursors. *J. Power Sources* 2012, 202, 284–290.
25. MacNeil, D.D.; Lu, Z.; Dahn, J.R. Structure and electrochemistry of LiO_2 ($0 \leq x \leq 1/2$). *J. Electrochem. Soc.* 2002, 149, 1332–1336.
26. Moorhead, R.Z.; Huq, A.; Goodenough, J.B.; Manthiram, A. Electronic and electrochemical properties of $\text{Li}_{1-x}\text{Mn}_{1.5}\text{Ni}_{0.5}\text{O}_4$ spinel cathodes as a function of lithium content and cation ordering. *Chem. Mater.* 2015, 27, 6934–6945.
27. Moorhead, R.Z.; Chemelewski, K.R.; Goodenough, J.B.; Manthiram, A. Magnetic measurements as a viable tool to assess the relative degrees of cation ordering and Mn^{3+} content in doped $\text{LiMn}_{1.5}\text{Ni}_{0.5}\text{O}_4$ spinel cathodes. *J. Mater. Chem. A* 2013, 1, 10745–10752.

28. Yan, J.; Huang, H.; Tong, J.; Li, W.; Liu, X.; Zhang, H.; Huang, H.; Zhou, W. Recent progress on the modification of high nickel content NCM: Coating, doping, and single crystallization. *Interdiscip. Mater.* 2022, 1, 330–353.
29. Wu, F.; Liu, N.; Chen, L.; Su, Y.; Tan, G.; Bao, L.; Zhang, Q.; Lu, Y.; Wang, J.; Chen, S.; et al. Improving the reversibility of the H2-H3 phase transitions for layered Ni-rich oxide cathode towards retarded structural transition and enhanced cycle stability. *Nano Energy* 2019, 59, 50–57.
30. Madec, L.; Xia, J.; Petibon, R.; Nelson, K.J.; Sun, J.-P.; Hill, I.G.; Dahn, J.R. Effect of sulfate electrolyte additives on LiNi_{1/3}Mn_{1/3}Co_{1/3}O₂/graphite pouch cell lifetime: Correlation between XPS surface studies and electrochemical test results. *J. Phys. Chem. C* 2014, 118, 29608–29622.
31. Zheng, H.; Sun, Q.; Liu, G.; Song, X.; Battaglia, V.S. Correlation between dissolution behavior and electrochemical cycling performance for LiNi_{1/3}Co_{1/3}Mn_{1/3}O₂-based cells. *J. Power Sources* 2012, 207, 134–140.
32. Hua, W.; Schwarz, B.; Knapp, M.; Senyshyn, A.; Missiul, A.; Mu, X.; Wang, S.; Kübel, C.; Binder, J.R.; Indris, S.; et al. (De)Lithiation mechanism of hierarchically layered LiNi_{1/3}Co_{1/3}Mn_{1/3}O₂ cathodes during high-voltage cycling. *J. Electrochem. Soc.* 2018, 166, A5025–A5032.
33. Zhang, X.; Mauger, A.; Lu, Q.; Groult, H.; Perrigaud, L.; Gendron, F.; Julien, C.M. Synthesis and characterization of LiNi_{1/3}Mn_{1/3}Co_{1/3}O₂ by wet-chemical method. *Electrochim. Acta* 2010, 55, 6440–6449.
34. Yan, P.; Zheng, J.; Zhang, J.G.; Wang, C. Atomic resolution structural and chemical imaging revealing the sequential migration of Ni, Co, and Mn upon the battery cycling of layered cathode. *Nano Lett.* 2017, 17, 3946–3951.
35. Wang, Q.; Feng, L.; Sun, J. A multi-component additive to improve the thermal stability of Li(Ni_{1/3}Co_{1/3}Mn_{1/3})O₂-based lithium ion batteries. *Energies* 2016, 9, 424.
36. Li, J.; Cameron, A.R.; Li, H.; Glazier, S.; Xiong, D.; Chatzidakis, M.; Allen, J.; Botton, G.A.; Dahn, J.R. Comparison of single crystal and polycrystalline LiNi_{0.5}Mn_{0.3}Co_{0.2}O₂ positive electrode materials for high voltage Li-ion cells. *J. Electrochem. Soc.* 2017, 164, A1534–A1544.
37. Berkes, B.B.; Schiele, A.; Sommer, H.; Brezesinski, T.; Janek, J. On the gassing behavior of lithium-ion batteries with NCM523 cathodes. *J. Solid State Electrochem.* 2016, 20, 2961–2967.
38. Zhang, Y.; Wang, Z.; Zhong, Y.; Wu, H.; Li, S.; Cheng, Q.; Guo, P. Coating for improving electrochemical performance of NCM523 cathode for lithium-ion batteries. *Ionics* 2020, 27, 13–20.
39. Li, J.; Huang, J.; Kong, X.; Zeng, J.; Zhao, J. The apparent capacity decay by kinetic degradation of LiNi_{0.5}Co_{0.2}Mn_{0.3}O₂ during cycling under the high upper-limit charging potential. *J. Power Sources* 2021, 496, 229856.

40. Jung, S.K.; Gwon, H.; Hong, J.; Park, K.Y.; Seo, D.H.; Kim, H.; Hyun, J.; Yang, W.; Kang, K. Understanding the degradation mechanisms of $\text{LiNi}_0.5\text{Co}_0.2\text{Mn}_0.3\text{O}_2$ cathode material in lithium ion batteries. *Adv. Energy Mater.* 2014, 4, 1300787.
41. Wu, Z.; Ji, S.; Zheng, J.; Hu, Z.; Xiao, S.; Wei, Y.; Zhuo, Z.; Lin, Y.; Yang, W.; Xu, K.; et al. Prelithiation activates $\text{Li}(\text{Ni}_0.5\text{Mn}_0.3\text{Co}_0.2)\text{O}_2$ for high capacity and excellent cycling stability. *Nano Lett.* 2015, 15, 5590–5596.
42. Noh, H.J.; Youn, S.; Yoon, C.S.; Sun, Y.K. Comparison of the structural and electrochemical properties of layered LiO_2 ($x = 1/3, 0.5, 0.6, 0.7, 0.8$ and 0.85) cathode material for lithium-ion batteries. *J. Power Sources* 2013, 233, 121–130.
43. Gu, M.; Belharouak, I.; Zheng, J.; Wu, H.; Xiao, J.; Genc, A.; Amine, K.; Thevuthasan, S.; Baer, D.R.; Zhang, J.G.; et al. Formation of the spinel phase in the layered composite cathode used in Li-ion batteries. *ACS Nano* 2013, 7, 760–767.
44. Lin, F.; Markus, I.M.; Nordlund, D.; Weng, T.C.; Asta, M.D.; Xin, H.L.; Doeff, M.M. Surface reconstruction and chemical evolution of stoichiometric layered cathode materials for lithium-ion batteries. *Nat. Commun.* 2014, 5, 3529.
45. Hua, W.; Schwarz, B.; Azmi, R.; Müller, M.; Dewi Darma, M.S.; Knapp, M.; Senyshyn, A.; Heere, M.; Missyul, A.; Simonelli, L.; et al. Lithium-ion (de)intercalation mechanism in core-shell layered $\text{Li}(\text{Ni},\text{Co},\text{Mn})\text{O}_2$ cathode materials. *Nano Energy* 2020, 78, 105231.
46. Cherkashinin, G.; Motzko, M.; Schulz, N.; Späth, T.; Jaegermann, W. Electron spectroscopy study of $\text{LiO}_2/\text{electrolyte}$ interface: Electronic structure, interface composition, and device implications. *Chem. Mater.* 2015, 27, 2875–2887.
47. Ming, J.; Kwak, W.J.; Youn, S.J.; Ming, H.; Hassoun, J.; Sun, Y.-K. Lithiation of an iron oxide-based anode for stable, high-capacity lithium-ion batteries of porous carbon- $\text{Fe}_3\text{O}_4/\text{LiO}_2$. *Energy Technol.* 2014, 2, 778–785.
48. Azmi, R.; Masoumi, M.; Ehrenberg, H.; Trouillet, V.; Bruns, M. Surface analytical characterization of $\text{LiNi}_{0.8-y}\text{Mn}_y\text{Co}_{0.2}\text{O}_2$ ($0 \leq y \leq 0.4$) compounds for lithium-ion battery electrodes. *Surf. Interface Anal.* 2018, 50, 1132–1137.
49. Huang, W.; Lin, C.; Zhang, M.; Li, S.; Chen, Z.; Zhao, W.; Zhu, C.; Zhao, Q.; Chen, H.; Pan, F. Revealing roles of Co and Ni in Mn-rich layered cathodes. *Adv. Energy Mater.* 2021, 11, 2102646.
50. Shim, J.H.; Kim, C.Y.; Cho, S.W.; Missiul, A.; Kim, J.-K.; Ahn, Y.J.; Lee, S. Effects of heat-treatment atmosphere on electrochemical performances of Ni-rich mixed-metal oxide ($\text{LiNi}_{0.80}\text{Co}_{0.15}\text{Mn}_{0.05}\text{O}_2$) as a cathode material for lithium ion battery. *Electrochim. Acta* 2014, 138, 15–21.
51. Lim, H.; Na, D.; Lee, C.R.; Seo, H.K.; Kwon, O.H.; Kim, J.K.; Seo, I. An integrated device of a lithium-ion battery combined with silicon solar cells. *Energies* 2021, 14, 6010.

52. Zhang, N.; Li, J.; Li, H.; Liu, A.; Huang, Q.; Ma, L.; Li, Y.; Dahn, J.R. Structural, electrochemical, and thermal properties of nickel-rich $\text{LiNi}_x\text{Mn}_y\text{Co}_z\text{O}_2$ materials. *Chem. Mater.* 2018, 30, 8852–8860.
53. Zhang, Y.; Cao, H.; Zhang, J.; Xia, B. Synthesis of $\text{LiNi}_{0.6}\text{Co}_{0.2}\text{Mn}_{0.2}\text{O}_2$ cathode material by a carbonate co-precipitation method and its electrochemical characterization. *Solid State Ionics* 2006, 177, 3303–3307.
54. Cao, H.; Zhang, Y.; Zhang, J.; Xia, B. Synthesis and electrochemical characteristics of layered $\text{LiNi}_{0.6}\text{Co}_{0.2}\text{Mn}_{0.2}\text{O}_2$ cathode material for lithium ion batteries. *Solid State Ionics* 2005, 176, 1207–1211.
55. Chen, Y.; Zhang, Y.; Chen, B.; Wang, Z.; Lu, C. An approach to application for $\text{LiNi}_{0.6}\text{Co}_{0.2}\text{Mn}_{0.2}\text{O}_2$ cathode material at high cutoff voltage by TiO_2 coating. *J. Power Sources* 2014, 256, 20–27.
56. Liang, L.; Du, K.; Peng, Z.; Cao, Y.; Duan, J.; Jiang, J.; Hu, G. Co-precipitation synthesis of $\text{Ni}_{0.6}\text{Co}_{0.2}\text{Mn}_{0.2}(\text{OH})_2$ precursor and characterization of $\text{LiNi}_{0.6}\text{Co}_{0.2}\text{Mn}_{0.2}\text{O}_2$ cathode material for secondary lithium batteries. *Electrochim. Acta* 2014, 130, 82–89.
57. Yue, P.; Wang, Z.; Li, X.; Xiong, X.; Wang, J.; Wu, X.; Guo, H. The enhanced electrochemical performance of $\text{LiNi}_{0.6}\text{Co}_{0.2}\text{Mn}_{0.2}\text{O}_2$ cathode materials by low temperature fluorine substitution. *Electrochim. Acta* 2013, 95, 112–118.
58. Ju, S.H.; Kang, I.S.; Lee, Y.S.; Shin, W.K.; Kim, S.; Shin, K.; Kim, D.W. Improvement of the cycling performance of $\text{LiNi}_{0.6}\text{Co}_{0.2}\text{Mn}_{0.2}\text{O}_2$ cathode active materials by a dual-conductive polymer coating. *ACS Appl. Mater. Interfaces* 2014, 6, 2546–2552.
59. Neudeck, S.; Walther, F.; Bergfeldt, T.; Suchomski, C.; Rohnke, M.; Hartmann, P.; Janek, J.; Brezesinski, T. Molecular surface modification of NCM622 cathode material using organophosphates for improved Li-ion battery full-cells. *ACS Appl. Mater. Interfaces* 2018, 10, 20487–20498.
60. Kim, A.Y.; Strauss, F.; Bartsch, T.; Teo, J.H.; Janek, J.; Brezesinski, T. Effect of surface carbonates on the cyclability of LiNbO_3 -coated NCM622 in all-solid-state batteries with lithium thiophosphate electrolytes. *Sci. Rep.* 2021, 11, 1–9.
61. Hua, W.; Wang, K.; Knapp, M.; Schwarz, B.; Wang, S.; Liu, H.; Lai, J.; Müller, M.; Schökel, A.; Missyul, A.; et al. Chemical and structural evolution during the synthesis of layered $\text{Li}(\text{Ni},\text{Co},\text{Mn})\text{O}_2$ oxides. *Chem. Mater.* 2020, 32, 4984–4997.
62. Kim, Y. Lithium nickel cobalt manganese oxide synthesized using alkali chloride flux: Morphology and performance as a cathode material for lithium ion batteries. *ACS Appl. Mater. Interfaces* 2012, 4, 2329–2333.

63. Lim, J.M.; Hwang, T.; Kim, D.; Park, M.S.; Cho, K.; Cho, M. Intrinsic origins of crack generation in Ni-rich $\text{LiNi}_0.8\text{Co}_0.1\text{Mn}_0.1\text{O}_2$ layered oxide cathode material. *Sci. Rep.* 2017, 7, 39669.
64. Kim, H.R.; Woo, S.G.; Kim, J.H.; Cho, W.; Kim, Y.J. Capacity fading behavior of Ni-rich layered cathode materials in Li-ion full cells. *J. Electroanal. Chem.* 2016, 782, 168–173.
65. Xi, Y.; Liu, Y.; Zhang, D.; Jin, S.; Zhang, R.; Jin, M. Comparative study of the electrochemical performance of $\text{LiNi}_0.5\text{Co}_0.2\text{Mn}_0.3\text{O}_2$ and $\text{LiNi}_0.8\text{Co}_0.1\text{Mn}_0.1\text{O}_2$ cathode materials for lithium ion batteries. *Solid State Ionics* 2018, 327, 27–31.
66. Huang, Y.; Wang, Z.X.; Li, X.H.; Guo, H.J.; Wang, J.X. Synthesis of $\text{Ni}_0.8\text{Co}_0.1\text{Mn}_0.1(\text{OH})_2$ precursor and electrochemical performance of $\text{LiNi}_0.8\text{Co}_0.1\text{Mn}_0.1\text{O}_2$ cathode material for lithium batteries. *Trans. Nonferrous Met. Soc. China* 2015, 25, 2253–2259.
67. Li, W.; Liu, X.; Xie, Q.; You, Y.; Chi, M.; Manthiram, A. Long-term cyclability of NCM-811 at high voltages in lithium-ion batteries: An in-depth diagnostic study. *Chem. Mater.* 2020, 32, 7796–7804.
68. Song, W.; Harlow, J.; Logan, E.; Hebecker, H.; Coon, M.; Molino, L.; Johnson, M.; Dahn, J.; Metzger, M. A Systematic study of electrolyte additives in single crystal and bimodal $\text{LiNi}_0.8\text{Mn}_0.1\text{Co}_0.1\text{O}_2$ /graphite pouch cells. *J. Electrochem. Soc.* 2021, 168, 090503.
69. Ryu, H.H.; Park, K.J.; Yoon, C.S.; Sun, Y.K. Capacity fading of Ni-rich LiO_2 ($0.6 \leq x \leq 0.95$) cathodes for high-energy-density lithium-ion batteries: Bulk or surface degradation? *Chem. Mater.* 2018, 30, 1155–1163.
70. Hu, J.P.; Sheng, H.; Deng, Q.; Ma, Q.; Liu, J.; Wu, X.W.; Liu, J.J.; Wu, Y.P. High-rate layered cathode of lithium-ion batteries through regulating three-dimensional agglomerated structure. *Energies* 2020, 13, 1602.
71. Heck, C.A.; von Horstig, M.W.; Huttner, F.; Mayer, J.K.; Haselrieder, W.; Kwade, A. Review—Knowledge-based process design for high quality production of NCM811 cathodes. *J. Electrochem. Soc.* 2020, 167, 160521.
72. Yoon, C.S.; Choi, M.H.; Lim, B.-B.; Lee, E.J.; Sun, Y.K. Review—High-capacity LiO_2 ($x = 0.1, 0.05, 0$) cathodes for next-generation Li-ion battery. *J. Electrochem. Soc.* 2015, 162, A2483–A2489.
73. Seong, W.M.; Cho, K.H.; Park, J.W.; Park, H.; Eum, D.; Lee, M.H.; Kim, I.S.; Lim, J.; Kang, K. Controlling residual lithium in high-nickel (>90 %) lithium layered oxides for cathodes in lithium-ion batteries. *Angew. Chem. Int. Ed.* 2020, 59, 18662–18669.
74. Song, S.H.; Hong, S.; Cho, M.; Yoo, J.G.; Min Jin, H.; Lee, S.H.; Avdeev, M.; Ikeda, K.; Kim, J.; Nam, S.C.; et al. Rational design of Li off-stoichiometric Ni-rich layered cathode materials for Li-ion batteries. *Chem. Eng. J.* 2022, 448, 137685.
75. Jun, D.W.; Yoon, C.S.; Kim, U.H.; Sun, Y.K. High-energy density core–shell structured LiO_2 cathode for lithium-ion batteries. *Chem. Mater.* 2017, 29, 5048–5052.

76. Park, K.J.; Jung, H.G.; Kuo, L.Y.; Kaghazchi, P.; Yoon, C.S.; Sun, Y.K. Improved cycling stability of LiO₂ through microstructure modification by boron doping for Li-ion batteries. *Adv. Energy Mater.* 2018, 8, 1301564.
77. Jamil, S.; Yue, L.; Li, C.; Fasehullah, M.; Aizaz Ud Din, M.; Yang, W.; Bao, S.; Xu, M. Significance of gallium doping for high Ni, low Co/Mn layered oxide cathode material. *Chem. Eng. J.* 2022, 441, 135821.
78. Park, N.Y.; Ryu, H.H.; Park, G.T.; Noh, T.C.; Sun, Y.K. Optimized Ni-rich NCMA cathode for electric vehicle batteries. *Adv. Energy Mater.* 2021, 11, 2003767.
79. Zhang, N.; Zaker, N.; Li, H.; Liu, A.; Inglis, J.; Jing, L.; Li, J.; Li, Y.; Botton, G.A.; Dahn, J.R. Cobalt-free nickel-rich positive electrode materials with a core-shell structure. *Chem. Mater.* 2019, 31, 10150–10160.
80. Li, H.; Cormier, M.; Zhang, N.; Inglis, J.; Li, J.; Dahn, J.R. Is cobalt needed in Ni-rich positive electrode materials for lithium ion batteries? *J. Electrochem. Soc.* 2019, 166, A429–A439.
81. Rathore, D.; Geng, C.; Zaker, N.; Hamam, I.; Liu, Y.; Xiao, P.; Botton, G.A.; Dahn, J.; Yang, C. Tungsten infused grain boundaries enabling universal performance enhancement of Co-free Ni-rich cathode materials. *J. Electrochem. Soc.* 2021, 168, 120514.
82. Su, L.; Jo, E.; Manthiram, A. Protection of cobalt-free LiNiO₂ from degradation with localized saturated electrolytes in lithium-metal batteries. *ACS Energy Lett.* 2022, 7, 2165–2172.
83. Liu, T.; Yu, L.; Liu, J.; Lu, J.; Bi, X.; Dai, A.; Li, M.; Li, M.; Hu, Z.; Ma, L.; et al. Understanding Co roles towards developing Co-free Ni-rich cathodes for rechargeable batteries. *Nat. Energy* 2021, 6, 277–286.
84. Mu, L.; Yang, Z.; Tao, L.; Waters, C.K.; Xu, Z.; Li, L.; Sainio, S.; Du, Y.; Xin, H.L.; Nordlund, D.; et al. The sensitive surface chemistry of Co-free, Ni-rich layered oxides: Identifying experimental conditions that influence characterization results. *J. Mater. Chem. A* 2020, 8, 17487–17497.
85. Li, N.; Sallis, S.; Papp, J.K.; McCloskey, B.D.; Yang, W.; Tong, W. Correlating the phase evolution and anionic redox in Co-free Ni-rich layered oxide cathodes. *Nano Energy* 2020, 78, 105365.
86. Aishova, A.; Park, G.T.; Yoon, C.S.; Sun, Y.K. Cobalt-free high-capacity Ni-rich layered LiO₂ cathode. *Adv. Energy Mater.* 2019, 10, 1903179.
87. Wang, X.; Ding, Y.L.; Deng, Y.P.; Chen, Z. Ni-rich/Co-poor layered cathode for automotive Li-ion batteries: Promises and challenges. *Adv. Energy Mater.* 2020, 10, 1903864.
88. Kim, S.; Na, S.; Kim, J.; Jun, T.H.; Oh, M.H.; Min, K.; Park, K. Multifunctional surface modification with Co-free spinel structure on Ni-rich cathode material for improved electrochemical performance. *J. Alloys Compd.* 2022, 918, 165454.

89. Wang, C.; Tan, L.; Yi, H.; Zhao, Z.; Yi, X.; Zhou, Y.; Zheng, J.; Wang, J.; Li, L. Unveiling the impact of residual Li conversion and cation ordering on electrochemical performance of Co-free Ni-rich cathodes. *Nano Res.* 2022, 15, 9038–9046.
90. Xi, Y.; Wang, M.; Xu, L.; Kheimeh Sari, H.M.; Li, W.; Hu, J.; Cao, Y.; Chen, L.; Wang, L.; Pu, X.; et al. A new Co-free Ni-rich $\text{LiNi}_0.8\text{Fe}_0.1\text{Mn}_0.1\text{O}_2$ cathode for low-cost Li-ion batteries. *ACS Appl. Mater. Interfaces* 2021, 13, 57341–57349.
91. Choi, J.U.; Voronina, N.; Sun, Y.K.; Myung, S.T. Recent progress and perspective of advanced high-energy Co-less Ni-rich cathodes for Li-ion batteries: Yesterday, today, and tomorrow. *Adv. Energy Mater.* 2020, 10.
92. Schipper, F.; Erickson, E.M.; Erk, C.; Shin, J.-Y.; Chesneau, F.F.; Aurbach, D. Review—Recent advances and remaining challenges for lithium ion battery cathodes. *J. Electrochem. Soc.* 2016, 164, A6220–A6228.
93. Liang, L.; Zhang, W.; Zhao, F.; Denis, D.K.; Zaman, F.u.; Hou, L.; Yuan, C. Surface/interface structure degradation of Ni-rich layered oxide cathodes toward lithium-ion batteries: Fundamental mechanisms and remedying strategies. *Adv. Mater. Interfaces* 2019, 7, 1901749.
94. Julien, C.M.; Mauger, A. NCA, NCM811, and the route to Ni-richer lithium-ion batteries. *Energies* 2020, 13, 6363.
95. Myung, S.T.; Maglia, F.; Park, K.J.; Yoon, C.S.; Lamp, P.; Kim, S.J.; Sun, Y.K. Nickel-rich layered cathode materials for automotive lithium-ion batteries: Achievements and perspectives. *ACS Energy Lett.* 2016, 2, 196–223.
96. Li, H.; Liu, A.; Zhang, N.; Wang, Y.; Yin, S.; Wu, H.; Dahn, J.R. An unavoidable challenge for Ni-rich positive electrode materials for lithium-ion batteries. *Chem. Mater.* 2019, 31, 7574–7583.
97. Li, W.; Asl, H.Y.; Xie, Q.; Manthiram, A. collapse of $\text{LiNi}_{1-x-y}\text{Co}_x\text{Mn}_y\text{O}_2$ lattice at deep charge irrespective of nickel content in lithium-ion batteries. *J. Am. Chem. Soc.* 2019, 141, 5097–5101.
98. Geldasa, F.T.; Kebede, M.A.; Shura, M.W.; Hone, F.G. Identifying surface degradation, mechanical failure, and thermal instability phenomena of high energy density Ni-rich NCM cathode materials for lithium-ion batteries: A review. *RSC Adv.* 2022, 12, 5891–5909.
99. Ko, D.S.; Park, J.H.; Yu, B.Y.; Ahn, D.; Kim, K.; Han, H.N.; Jeon, W.S.; Jung, C.; Manthiram, A. Degradation of high-nickel-layered oxide cathodes from surface to bulk: A comprehensive structural, chemical, and electrical analysis. *Adv. Energy Mater.* 2020, 10, 2001035.
100. Sun, H.H.; Kim, U.H.; Park, J.H.; Park, S.W.; Seo, D.H.; Heller, A.; Mullins, C.B.; Yoon, C.S.; Sun, Y.K. Transition metal-doped Ni-rich layered cathode materials for durable Li-ion batteries. *Nat. Commun.* 2021, 12, 1–11.

101. Julien, C.; Nazri, G.A.; Rougier, A. Electrochemical performances of layered $\text{LiM}_{1-y}\text{M}'_y\text{O}_2$ ($\text{M} = \text{Ni}, \text{Co}$; $\text{M}' = \text{Mg}, \text{Al}, \text{B}$) oxides in lithium batteries. *Solid State Ionics* 2000, 135, 121–130.
102. Samarasingha, P.B.; Wijayasinghe, A.; Behm, M.; Dissanayake, L.; Lindbergh, G. Development of cathode materials for lithium ion rechargeable batteries based on the system $\text{Li}(\text{Ni}_{1/3}\text{Mn}_{1/3}\text{Co}_{(1/3-x)}\text{M}_x)\text{O}_2$, ($\text{M} = \text{Mg}, \text{Fe}, \text{Al}$ and $x = 0.00$ to 0.33). *Solid State Ionics* 2014, 268, 226–230.
103. Sattar, T.; Lee, S.H.; Sim, S.J.; Jin, B.S.; Kim, H.S. Effect of Mg-doping on the electrochemical performance of $\text{LiNi}_{0.84}\text{Co}_{0.11}\text{Mn}_{0.05}\text{O}_2$ cathode for lithium ion batteries. *Int. J. Hydrogen Energy* 2020, 45, 19567–19576.
104. Zhou, F.; Zhao, X.; Lu, Z.; Jiang, J.; Dahn, J.R. The effect of Al substitution on the reactivity of delithiated $\text{LiNi}_{1/3}\text{Mn}_{1/3}\text{Co}_{(1/3-z)}\text{Al}_z\text{O}_2$ with non-aqueous electrolyte. *Electrochem. Commun.* 2008, 10, 1168–1171.
105. Zhang, M.; Wang, C.; Zhang, J.; Li, G.; Gu, L. Preparation and electrochemical characterization of La and Al Co-doped NCM811 cathode materials. *ACS Omega* 2021, 6, 16465–16471.
106. Schipper, F.; Dixit, M.; Kovacheva, D.; Talianker, M.; Haik, O.; Grinblat, J.; Erickson, E.M.; Ghanty, C.; Major, D.T.; Markovsky, B.; et al. Stabilizing nickel-rich layered cathode materials by a high-charge cation doping strategy: Zirconium-doped $\text{LiNi}_{0.6}\text{Co}_{0.2}\text{Mn}_{0.2}\text{O}_2$. *J. Mater. Chem. A* 2016, 4, 16073–16084.
107. Han, B.; Xu, S.; Zhao, S.; Lin, G.; Feng, Y.; Chen, L.; Ivey, D.G.; Wang, P.; Wei, W. Enhancing the structural stability of Ni-rich layered oxide cathodes with a preformed Zr-concentrated defective nanolayer. *ACS Appl. Mater. Interfaces* 2018, 10, 39599–39607.
108. Gao, S.; Zhan, X.; Cheng, Y.T. Structural, electrochemical and Li-ion transport properties of Zr-modified $\text{LiNi}_{0.8}\text{Co}_{0.1}\text{Mn}_{0.1}\text{O}_2$ positive electrode materials for Li-ion batteries. *J. Power Sources* 2019, 410–411, 45–52.
109. Du, R.; Bi, Y.; Yang, W.; Peng, Z.; Liu, M.; Liu, Y.; Wu, B.; Yang, B.; Ding, F.; Wang, D. Improved cyclic stability of $\text{LiNi}_{0.8}\text{Co}_{0.1}\text{Mn}_{0.1}\text{O}_2$ via Ti substitution with a cut-off potential of 4.5V. *Ceram. Int.* 2015, 41, 7133–7139.
110. Sun, H.; Cao, Z.; Wang, T.; Lin, R.; Li, Y.; Liu, X.; Zhang, L.; Lin, F.; Huang, Y.; Luo, W. Enabling high rate performance of Ni-rich layered oxide cathode by uniform titanium doping. *Mater. Today Energy* 2019, 13, 145–151.
111. Zhang, D.; Liu, Y.; Wu, L.; Feng, L.; Jin, S.; Zhang, R.; Jin, M. Effect of Ti ion doping on electrochemical performance of Ni-rich $\text{LiNi}_{0.8}\text{Co}_{0.1}\text{Mn}_{0.1}\text{O}_2$ cathode material. *Electrochim. Acta* 2019, 328, 135086.
112. Jia, X.; Yan, M.; Zhou, Z.; Chen, X.; Yao, C.; Li, D.; Chen, D.; Chen, Y. Nd-doped $\text{LiNi}_{0.5}\text{Co}_{0.2}\text{Mn}_{0.3}\text{O}_2$ as a cathode material for better rate capability in high voltage cycling of Li-

- ion batteries. *Electrochim. Acta* 2017, 254, 50–58.
113. Liu, S.; Chen, X.; Zhao, J.; Su, J.; Zhang, C.; Huang, T.; Wu, J.; Yu, A. Uncovering the role of Nb modification in improving the structure stability and electrochemical performance of $\text{LiNi}_0.6\text{Co}_0.2\text{Mn}_0.2\text{O}_2$ cathode charged at higher voltage of 4.5 V. *J. Power Sources* 2018, 374, 149–157.
114. Su, Y.; Yang, Y.; Chen, L.; Lu, Y.; Bao, L.; Chen, G.; Yang, Z.; Zhang, Q.; Wang, J.; Chen, R.; et al. Improving the cycling stability of Ni-rich cathode materials by fabricating surface rock salt phase. *Electrochim. Acta* 2018, 292, 217–226.
115. Breuer, O.; Chakraborty, A.; Liu, J.; Kravchuk, T.; Burstein, L.; Grinblat, J.; Kauffman, Y.; Gladkih, A.; Nayak, P.; Tsubery, M.; et al. Understanding the role of minor molybdenum doping in $\text{LiNi}_0.5\text{Co}_0.2\text{Mn}_0.3\text{O}_2$ electrodes: From structural and surface analyses and theoretical modeling to practical electrochemical cells. *ACS Appl. Mater. Interfaces* 2018, 10, 29608–29621.
116. Li, L.J.; Wang, Z.X.; Liu, Q.C.; Ye, C.; Chen, Z.Y.; Gong, L. Effects of chromium on the structural, surface chemistry and electrochemical of layered $\text{LiNi}_{0.8-x}\text{Co}_{0.1}\text{Mn}_{0.1}\text{Cr}_x\text{O}_2$. *Electrochim. Acta* 2012, 77, 89–96.
117. Yue, P.; Wang, Z.; Wang, J.; Guo, H.; Xiong, X.; Li, X. Effect of fluorine on the electrochemical performance of spherical $\text{LiNi}_0.8\text{Co}_0.1\text{Mn}_0.1\text{O}_2$ cathode materials via a low temperature method. *Powder Technol.* 2013, 237, 623–626.
118. Binder, J.O.; Culver, S.P.; Pinedo, R.; Weber, D.A.; Friedrich, M.S.; Gries, K.I.; Volz, K.; Zeier, W.G.; Janek, J. Investigation of fluorine and nitrogen as anionic dopants in nickel-rich cathode materials for lithium-ion batteries. *ACS Appl. Mater. Interfaces* 2018, 10, 44452–44462.
119. Li, C.; Kan, W.H.; Xie, H.; Jiang, Y.; Zhao, Z.; Zhu, C.; Xia, Y.; Zhang, J.; Xu, K.; Mu, D.; et al. Inducing favorable cation antisite by doping halogen in Ni-rich layered cathode with ultrahigh stability. *Adv. Sci. News* 2019, 6, 1801406.
120. Kim, H.; Kim, S.B.; Park, D.H.; Park, K.W. Fluorine-doped $\text{LiNi}_0.8\text{Mn}_0.1\text{Co}_0.1\text{O}_2$ cathode for high-performance lithium-ion batteries. *Energies* 2020, 13, 4808.
121. Lee, S.H.; Jin, B.S.; Kim, H.S. Superior performances of B-doped $\text{LiNi}_0.84\text{Co}_0.10\text{Mn}_0.06\text{O}_2$ cathode for advanced LIBs. *Sci. Rep.* 2019, 9, 1–7.
122. Roitzheim, C.; Kuo, L.Y.; Sohn, Y.J.; Finsterbusch, M.; Möller, S.; Sebold, D.; Valencia, H.; Meledina, M.; Mayer, J.; Breuer, U.; et al. Boron in Ni-rich NCM811 cathode material: Impact on atomic and microscale properties. *ACS Appl. Energy Mater.* 2021, 5, 524–538.
123. Weigel, T.; Schipper, F.; Erickson, E.M.; Susai, F.A.; Markovsky, B.; Aurbach, D. Structural and electrochemical aspects of $\text{LiNi}_0.8\text{Co}_0.1\text{Mn}_0.1\text{O}_2$ cathode materials doped by various cations. *ACS Energy Lett.* 2019, 4, 508–516.

124. Zhang, Y.; Li, H.; Liu, J.; Zhang, J.; Cheng, F.; Chen, J. LiNi_{0.90}Co_{0.07}Mg_{0.03}O₂ cathode materials with Mg-concentration gradient for rechargeable lithium-ion batteries. *J. Mater. Chem. A* 2019, 7, 20958–20964.
125. Liu, T.; Yu, L.; Lu, J.; Zhou, T.; Huang, X.; Cai, Z.; Dai, A.; Gim, J.; Ren, Y.; Xiao, X.; et al. Rational design of mechanically robust Ni-rich cathode materials via concentration gradient strategy. *Nat. Commun.* 2021, 12, 1–10.
126. Zhang, H.; Xu, J.; Zhang, J. Surface-coated LiNi_{0.8}Co_{0.1}Mn_{0.1}O₂ (NCM811) cathode materials by Al₂O₃, ZrO₂, and Li₂O-2B₂O₃ thin-layers for improving the performance of lithium ion batteries. *Front. Mater.* 2019, 6, 309.
127. Karayaylali, P.; Tatara, R.; Zhang, Y.; Chan, K.L.; Yu, Y.; Giordano, L.; Maglia, F.; Jung, R.; Lund, I.; Shao, H.Y. Editors' Choice—Coating-dependent electrode-electrolyte interface for Ni-rich positive electrodes in Li-ion batteries. *J. Electrochem. Soc.* 2019, 166, A1022–A1030.
128. Cho, W.; Kim, S.M.; Song, J.H.; Yim, T.; Woo, S.G.; Lee, K.W.; Kim, J.S.; Kim, Y.J. Improved electrochemical and thermal properties of nickel rich LiNi_{0.6}Co_{0.2}Mn_{0.2}O₂ cathode materials by SiO₂ coating. *J. Power Sources* 2015, 282, 45–50.
129. Liang, L.; Hu, G.; Jiang, F.; Cao, Y. Electrochemical behaviours of SiO₂-coated LiNi_{0.8}Co_{0.1}Mn_{0.1}O₂ cathode materials by a novel modification method. *J. Alloys Compd.* 2016, 657, 570–581.
130. Dou, L.; Hu, P.; Shang, C.; Wang, H.; Xiao, D.; Ahuja, U.; Aifantis, K.; Zhang, Z.; Huang, Z. Enhanced electrochemical performance of LiNi_{0.8}Co_{0.1}Mn_{0.1}O₂ with SiO₂ surface coating via homogeneous precipitation. *ChemElectroChem* 2021, 8, 4321–4327.
131. Liu, W.; Gao, F.; Zang, Y.; Qu, J.; Xu, J.; Ji, S.; Huo, Y.; Qiu, J. Boosting cycle stability of NCM811 cathode material via 2D Mg-Al-LDO nanosheet coating for lithium-ion battery. *J. Alloys Compd.* 2021, 867, 159079.
132. Zhu, W.; Huang, X.; Liu, T.; Xie, Z.; Wang, Y.; Tian, K.; Bu, L.; Wang, H.; Gao, L.; Zhao, J. Ultrathin Al₂O₃ coating on LiNi_{0.8}Co_{0.1}Mn_{0.1}O₂ cathode material for enhanced cycleability at extended voltage ranges. *Coatings* 2019, 9, 92.
133. Feng, Y.; Xu, H.; Wang, B.; Wang, S.; Ai, L.; Li, S. Enhanced electrochemical performance of LiNi_{0.8}Co_{0.1}Mn_{0.1}O₂ cathode materials by Al₂O₃ coating. *J. Electrochem. Energy Convers. Storage* 2021, 18, 1–14.
134. Neudeck, S.; Strauss, F.; Garcia, G.; Wolf, H.; Janek, J.; Hartmann, P.; Brezesinski, T. Room temperature, liquid-phase Al₂O₃ surface coating approach for Ni-rich layered oxide cathode material. *Chem. Commun. (Camb.)* 2019, 55, 2174–2177.
135. Liu, W.; Li, X.; Xiong, D.; Hao, Y.; Li, J.; Kou, H.; Yan, B.; Li, D.; Lu, S.; Koo, A.; et al. Significantly improving cycling performance of cathodes in lithium ion batteries: The effect of Al₂O₃ and LiAlO₂

- coatings on $\text{LiNi}_{0.6}\text{Co}_{0.2}\text{Mn}_{0.2}\text{O}_2$. *Nano Energy* 2018, 44, 111–120.
136. Schipper, F.; Bouzaglo, H.; Dixit, M.; Erickson, E.M.; Weigel, T.; Talianker, M.; Grinblat, J.; Burstein, L.; Schmidt, M.; Lampert, J.; et al. From surface ZrO_2 coating to bulk Zr doping by high temperature annealing of nickel-rich lithiated oxides and their enhanced electrochemical performance in lithium ion batteries. *Adv. Energy Mater.* 2018, 8, 1701682.
137. Woo, S.G.; Han, J.H.; Kim, K.J.; Kim, J.H.; Yu, J.S.; Kim, Y.J. Surface modification by sulfated zirconia on high-capacity nickel-based cathode materials for Li-ion batteries. *Electrochim. Acta* 2015, 153, 115–121.
138. Herzog, M.J.; Esken, D.; Janek, J. Improved Cycling Performance of High-Nickel NMC by dry powder coating with nanostructured fumed Al_2O_3 , TiO_2 , and ZrO_2 : A comparison. *Batter. Supercaps* 2021, 4, 1003–1017.
139. Tubtimkuna, S.; Phattharasupakun, N.; Bunyanidhi, P.; Sawangphruk, M. Diffusion of zirconium (iv) ions from coated thick zirconium oxide shell to the bulk structure of Ni-rich NMC811 cathode leading to high-performance 18650 cylindrical Li-ion batteries. *Adv. Mater. Technol.* 2022.
140. Li, W.; Li, Y.; Yang, L.; Zhu, J.; Guo, J.; Yang, J.C. Enhanced the electrochemical performances of $\text{LiNi}_{0.7}\text{Co}_{0.15}\text{Mn}_{0.15}\text{O}_2$ cathodes by the hybrid ZrO_2 - Li_2ZrO_3 layer. *Ionics* 2020, 27, 479–489.
141. Jo, S.J.; Hwang, D.Y.; Lee, S.H. Use of zirconium dual-modification on the $\text{LiNi}_{0.8}\text{Co}_{0.1}\text{Mn}_{0.1}\text{O}_2$ cathode for improved electrochemical performances of lithium-ion batteries. *ACS Appl. Energy Mater.* 2021, 4, 3693–3700.
142. Kim, H.; Jang, J.; Byun, D.; Kim, H.S.; Choi, W. Selective TiO_2 nanolayer coating by polydopamine modification for highly stable Ni-rich layered oxides. *ChemSusChem* 2019, 12, 5253–5264.
143. Hwang, D.-Y.; Sim, S.-J.; Jin, B.-S.; Kim, H.-S.; Lee, S.-H. Suppressed microcracking and F penetration of Ni-rich layered cathode via the combined effects of titanium dioxide doping and coating. *ACS Appl. Energy Mater.* 2021, 4, 1743–1751.
144. Moryson, Y.; Walther, F.; Sann, J.; Mogwitz, B.; Ahmed, S.; Burkhardt, S.; Chen, L.; Klar, P.J.; Volz, K.; Fearn, S.; et al. Analyzing nanometer-thin cathode particle coatings for lithium-ion batteries—The example of TiO_2 on NCM622. *ACS Appl. Energy Mater.* 2021, 4, 7168–7181.
145. Xi, X.; Fan, Y.; Liu, Y.; Chen, Z.; Zou, J.; Zhu, S. Enhanced cyclic stability of NCM-622 cathode by Ti^{3+} doped TiO_2 coating. *J. Alloys Compd.* 2021, 872, 159664.
146. Razmjoo Kholari, M.A.; Azar, M.K.; Esmaili, M.; Malekpour, N.; Hosseini-Hosseiniabad, S.M.; Moakhar, R.S.; Dolati, A.; Ramakrishna, S. Electrochemical performance and elevated temperature properties of the TiO_2 -coated LiO_2 cathode material for high-safety li-ion batteries. *ACS Appl. Energy Mater.* 2021, 4, 5304–5315.

147. Peng, Z.; Li, T.; Zhang, Z.; Du, K.; Hu, G.; Cao, Y. Surface architecture decoration on enhancing properties of $\text{LiNi}_{0.8}\text{Co}_{0.1}\text{Mn}_{0.1}\text{O}_2$ with building bi-phase Li_3PO_4 and AlPO_4 by $\text{Al}(\text{H}_2\text{PO}_4)_3$ treatment. *Electrochim. Acta* 2020, 338, 135870.
148. Wu, Y.; Ming, H.; Li, M.; Zhang, J.; Wahyudi, W.; Xie, L.; He, X.; Wang, J.; Wu, Y.; Ming, J. New organic complex for lithium layered oxide modification: Ultrathin coating, high-voltage, and safety performances. *ACS Energy Lett.* 2019, 4, 656–665.
149. Zha, G.; Luo, Y.; Hu, N.; Ouyang, C.; Hou, H. Surface modification of the $\text{LiNi}_{0.8}\text{Co}_{0.1}\text{Mn}_{0.1}\text{O}_2$ cathode material by coating with FePO_4 with a yolk-shell structure for improved electrochemical performance. *ACS Appl. Mater. Interfaces* 2020, 12, 36046–36053.
150. Min, K.; Park, K.; Park, S.Y.; Seo, S.W.; Choi, B.; Cho, E. Improved electrochemical properties of $\text{LiNi}_{0.91}\text{Co}_{0.06}\text{Mn}_{0.03}\text{O}_2$ cathode material via Li-reactive coating with metal phosphates. *Sci. Rep.* 2017, 7, 1–10.
151. Lee, D.J.; Scrosati, B.; Sun, Y.K. $\text{Ni}_3(\text{PO}_4)_2$ -coated LiO_2 lithium battery electrode with improved cycling performance at 55 °C. *J. Power Sources* 2011, 196, 7742–7746.
152. Sattar, T.; Lee, S.H.; Sim, S.J.; Jin, B.S.; Kim, H.S. Understanding the combined effect of Ca doping and phosphate coating on Ni-rich $\text{LiNi}_{0.91}\text{Co}_{0.06}\text{Mn}_{0.03}\text{O}_2$ cathode material for Li-ion batteries. *Electrochim. Acta* 2021, 399, 139417.
153. Xu, L.; Zhou, F.; Liu, B.; Zhou, H.; Zhang, Q.; Kong, J.; Wang, Q. Progress in preparation and modification of $\text{LiNi}_{0.6}\text{Mn}_{0.2}\text{Co}_{0.2}\text{O}_2$ cathode material for high energy density li-ion batteries. *Int. J. Electrochem.* 2018, 2018, 1–12.
154. Cho, W.; Kim, S.M.; Lee, K.W.; Song, J.H.; Jo, Y.N.; Yim, T.; Kim, H.; Kim, J.S.; Kim, Y.J. Investigation of new manganese orthophosphate $\text{Mn}_3(\text{PO}_4)_2$ coating for nickel-rich $\text{LiNi}_{0.6}\text{Co}_{0.2}\text{Mn}_{0.2}\text{O}_2$ cathode and improvement of its thermal properties. *Electrochim. Acta* 2016, 198, 77–83.
155. Akella, S.H.; Taragin, S.; Wang, Y.; Aviv, H.; Kozen, A.C.; Zysler, M.; Wang, L.; Sharon, D.; Lee, S.B.; Noked, M. Improvement of the electrochemical performance of $\text{LiNi}_{0.8}\text{Co}_{0.1}\text{Mn}_{0.1}\text{O}_2$ via atomic layer deposition of lithium-rich zirconium phosphate coatings. *ACS Appl. Mater. Interfaces* 2021, 13, 61733–61741.
156. Hu, G.; Zhang, Z.; Li, T.; Gan, Z.; Du, K.; Peng, Z.; Xia, J.; Tao, Y.; Cao, Y. In Situ Surface Modification for Improving the Electrochemical Performance of Ni-Rich Cathode Materials by Using ZrP_2O_7 . *ChemSusChem* 2020, 13, 1603–1612.
157. Zhao, Z.; Wen, Z.; Liu, X.; Yang, H.; Chen, S.; Li, C.; Lv, H.; Wu, F.; Wu, B.; Mu, D. Tuning a compatible interface with LLZTO integrated on cathode material for improving NCM811/LLZTO solid-state battery. *Chem. Eng. J.* 2021, 405, 127031.

158. Jo, C.H.; Cho, D.H.; Noh, H.J.; Yashiro, H.; Sun, Y.K.; Myung, S.T. An effective method to reduce residual lithium compounds on Ni-rich LiO₂ active material using a phosphoric acid derived Li₃PO₄ nanolayer. *Nano Res.* 2014, 8, 1464–1479.
159. Fan, Q.; Yang, S.; Liu, J.; Liu, H.; Lin, K.; Liu, R.; Hong, C.; Liu, L.; Chen, Y.; An, K.; et al. Mixed-conducting interlayer boosting the electrochemical performance of Ni-rich layered oxide cathode materials for lithium ion batteries. *J. Power Sources* 2019, 421, 91–99.
160. Li, J.; Liu, Y.; Yao, W.; Rao, X.; Zhong, S.; Qian, L. Li₂TiO₃ and Li₂ZrO₃ co-modification LiNi_{0.8}Co_{0.1}Mn_{0.1}O₂ cathode material with improved high-voltage cycling performance for lithium-ion batteries. *Solid State Ionics* 2020, 349, 115292.
161. Song, B.; Li, W.; Oh, S.M.; Manthiram, A. Long-life nickel-rich layered oxide cathodes with a uniform Li₂ZrO₃ surface coating for lithium-ion batteries. *ACS Appl. Mater. Interfaces* 2017, 9, 9718–9725.
162. Zhao, C.; Liu, Z.Q.; Weng, W.; Wu, M.; Yan, X.Y.; Yang, J.; Lu, H.M.; Yao, X.Y. Stabilized cathode/sulfide solid electrolyte interface via Li₂ZrO₃ coating for all-solid-state batteries. *Rare Met.* 2022, 41, 3639–3645.
163. Yang, J.; Ren, K.; Hong, M.; Wang, T.; Wang, D.; Wang, T.; Wang, H. New insight into lattice variations of Ni-rich NMC811 cathode induced by Li₂ZrO₃ coating. *Mater. Technol.* 2021, 37, 1926–1935.
164. Yang, G.; Pan, K.; Lai, F.; Wang, Z.; Chu, Y.; Yang, S.; Han, J.; Wang, H.; Zhang, X.; Li, Q. Integrated co-modification of PO₄³⁻-polyanion doping and Li₂TiO₃ coating for Ni-rich layered LiNi_{0.6}Co_{0.2}Mn_{0.2}O₂ cathode material of Lithium-Ion batteries. *Chem. Eng. J.* 2021, 421, 129964.
165. Wang, J.; Yu, Y.; Li, B.; Fu, T.; Xie, D.; Cai, J.; Zhao, J. Improving the electrochemical properties of LiNi_(0.5)Co_(0.2)Mn_(0.3)O₂ at 4.6 V cutoff potential by surface coating with Li₂TiO₃ for lithium-ion batteries. *Phys. Chem. Chem. Phys.* 2015, 17, 32033–32043.
166. Liu, M.; Zhou, J.; Cheng, T.; Feng, Z.; Qin, Y.; Guo, B. Dual design of the surface via an ion conductor coating and in situ electrochemical diffusion enabling a long life for a Ni-rich cathode. *ACS Appl. Energy Mater.* 2022, 5, 9181–9188.
167. Jan, S.S.; Nurgul, S.; Shi, X.; Xia, H.; Pang, H. Improvement of electrochemical performance of LiNi_{0.8}Co_{0.1}Mn_{0.1}O₂ cathode material by graphene nanosheets modification. *Electrochim. Acta* 2014, 149, 86–93.
168. Son, I.H.; Park, J.H.; Park, S.; Park, K.; Han, S.; Shin, J.; Doo, S.G.; Hwang, Y.; Chang, H.; Choi, J.W. Graphene balls for lithium rechargeable batteries with fast charging and high volumetric energy densities. *Nat. Commun.* 2017, 8, 1561.

169. Luu, N.S.; Lim, J.-M.; Torres-Castanedo, C.G.; Park, K.-Y.; Moazzen, E.; He, K.; Meza, P.E.; Li, W.; Downing, J.R.; Hu, X.; et al. Elucidating and mitigating high-voltage interfacial chemomechanical degradation of nickel-rich lithium-ion battery cathodes via conformal graphene coating. *ACS Appl. Energy Mater.* 2021, 4, 11069–11079.
170. Shim, J.H.; Kim, Y.M.; Park, M.; Kim, J.; Lee, S. Reduced graphene oxide-wrapped nickel-rich cathode materials for lithium ion batteries. *ACS Appl. Mater. Interfaces* 2017, 9, 18720–18729.
171. Ning, R.; Yuan, K.; Zhang, K.; Shen, C.; Xie, K. A scalable snowballing strategy to construct uniform rGO-wrapped $\text{LiNi}_0.8\text{Co}_0.1\text{Mn}_0.1\text{O}_2$ with enhanced processability and electrochemical performance. *Appl. Surf. Sci.* 2021, 542, 148663.
172. Xu, G.L.; Liu, Q.; Lau, K.K.S.; Liu, Y.; Liu, X.; Gao, H.; Zhou, X.; Zhuang, M.; Ren, Y.; Li, J.; et al. Building ultraconformal protective layers on both secondary and primary particles of layered lithium transition metal oxide cathodes. *Nat. Energy* 2019, 4, 484–494.
173. Sun, Z.; Li, Z.; Gao, L.; Zhao, X.; Han, D.; Gan, S.; Guo, S.; Niu, L. Grafting benzenediazonium tetrafluoroborate onto $\text{LiNi}_x\text{Co}_y\text{Mn}_z\text{O}_2$ materials achieves subzero-temperature high-capacity lithium-ion storage via a diazonium soft-chemistry method. *Adv. Energy Mater.* 2018, 9, 1802946.
174. Diao, H.; Jia, M.; Zhao, N.; Guo, X. $\text{LiNi}_0.6\text{Co}_0.2\text{Mn}_0.2\text{O}_2$ cathodes coated with dual-conductive polymers for high-rate and long-life solid-state lithium batteries. *ACS Appl. Mater. Interfaces* 2022, 14, 24929–24937.
175. Gan, Q.; Qin, N.; Zhu, Y.; Huang, Z.; Zhang, F.; Gu, S.; Xie, J.; Zhang, K.; Lu, L.; Lu, Z. Polyvinylpyrrolidone-induced uniform surface-conductive polymer coating endows Ni-rich $\text{LiNi}_0.8\text{Co}_0.1\text{Mn}_0.1\text{O}_2$ with enhanced cyclability for lithium-ion batteries. *ACS Appl. Mater. Interfaces* 2019, 11, 12594–12604.
176. Fan, Q.; Lin, K.; Shi, Z.; Guan, S.; Chen, J.; Feng, S.; Liu, L. Constructing high conductive composite coating with tin and polypyrrole to improve the performance of $\text{LiNi}_0.8\text{Co}_0.1\text{Mn}_0.1\text{O}_2$ at high cutoff voltage of 4.5 V. *ACS Appl. Energy Mater.* 2021, 4, 10012–10024.
177. Yu, H.; Zhu, H.; Yang, Z.; Liu, M.; Jiang, H.; Li, C. Bulk Mg-doping and surface polypyrrole-coating enable high-rate and long-life for Ni-rich layered cathodes. *Chem. Eng. J.* 2021, 412, 128625.
178. Sun, Y.K.; Myung, S.T.; Park, B.C.; Prakash, J.; Belharouak, I.; Amine, K. High-energy cathode material for long-life and safe lithium batteries. *Nat. Mater.* 2009, 8, 320–324.
179. Kim, U.H.; Ryu, H.H.; Kim, J.H.; Mücke, R.; Kaghazchi, P.; Yoon, C.S.; Sun, Y.K. Microstructure-controlled Ni-rich cathode material by microscale compositional partition for next-generation electric vehicles. *Adv. Energy Mater.* 2019, 9, 1803902.
180. Ryu, H.M.; Kim, M.Y.; Jung, H.Y.; Lim, J.S.; Kim, Y.A.; Kim, H.S. Fabrication and electrochemical behavior of thin composite solid electrolyte for all-solid lithium batteries. *Ionics* 2020, 26, 2863–2874.

181. Cheng, F.; Zhang, X.; Qiu, Y.; Zhang, J.; Liu, Y.; Wei, P.; Ou, M.; Sun, S.; Xu, Y.; Li, Q.; et al. Tailoring electrolyte to enable high-rate and super-stable Ni-rich NCM cathode materials for Li-ion batteries. *Nano Energy* 2021, 88, 106301.
182. Shen, L.; Wu, H.B.; Liu, F.; Shen, J.; Mo, R.; Chen, G.; Tan, G.; Chen, J.; Kong, X.; Lu, X.; et al. Particulate anion sorbents as electrolyte additives for lithium batteries. *Adv. Funct. Mater.* 2020, 30, 2003055.
183. Shi, X.; Zheng, T.; Xiong, J.; Zhu, B.; Cheng, Y.J.; Xia, Y. Stable electrode/electrolyte interface for high-voltage NCM523 cathode constructed by synergistic positive and passive approaches. *ACS Appl. Mater. Interfaces* 2021, 13, 57107–57117.
184. Pham, H.Q.; Thi Tran, Y.H.; Han, J.; Song, S.W. Roles of nonflammable organic liquid electrolyte in stabilizing the interface of the $\text{LiNi}_0.8\text{Co}_0.1\text{Mn}_0.1\text{O}_2$ Cathode at 4.5 V and improving the battery performance. *J. Phys. Chem. C* 2019, 124, 175–185.
185. Lee, Y.; Lee, T.K.; Kim, S.; Lee, J.; Ahn, Y.; Kim, K.; Ma, H.; Park, G.; Lee, S.M.; Kwak, S.K.; et al. Fluorine-incorporated interface enhances cycling stability of lithium metal batteries with Ni-rich NCM cathodes. *Nano Energy* 2020, 67, 104309.
186. Wu, Q.; Mao, S.; Wang, Z.; Tong, Y.; Lu, Y. Improving $\text{LiNi}_x\text{Co}_y\text{Mn}_{1-x-y}\text{O}_2$ cathode electrolyte interface under high voltage in lithium ion batteries. *Nano Sel.* 2020, 1, 111–134.
187. An, F.; Zhao, H.; Zhou, W.; Ma, Y.; Li, P. S-containing and Si-containing compounds as highly effective electrolyte additives for SiO_x -based anodes/NCM 811 cathodes in lithium ion cells. *Sci. Rep.* 2019, 9, 1–16.
188. Yan, P.; Zheng, J.; Liu, J.; Wang, B.; Cheng, X.; Zhang, Y.; Sun, X.; Wang, C.; Zhang, J.G. Tailoring grain boundary structures and chemistry of Ni-rich layered cathodes for enhanced cycle stability of lithium-ion batteries. *Nat. Energy* 2018, 3, 600–605.
189. Xu, S.; Sun, Z.; Sun, C.; Li, F.; Chen, K.; Zhang, Z.; Hou, G.; Cheng, H.M.; Li, F. Homogeneous and fast ion conduction of PEO-based solid-state electrolyte at low temperature. *Adv. Funct. Mater.* 2020, 30, 2007172.
190. Kitsche, D.; Tang, Y.; Ma, Y.; Goonetilleke, D.; Sann, J.; Walther, F.; Bianchini, M.; Janek, J.; Brezesinski, T. High performance all-solid-state batteries with a Ni-rich NCM cathode coated by atomic layer deposition and lithium thiophosphate solid electrolyte. *ACS Appl. Energy Mater.* 2021, 4, 7338–7345.
191. Walther, F.; Strauss, F.; Wu, X.; Mogwitz, B.; Hertle, J.; Sann, J.; Rohnke, M.; Brezesinski, T.; Janek, J. The working principle of a $\text{Li}_2\text{CO}_3/\text{LiNbO}_3$ coating on NCM for thiophosphate-based all-solid-state batteries. *Chem. Mater.* 2021, 33, 2110–2125.
192. Zhao, C.Z.; Zhao, Q.; Liu, X.; Zheng, J.; Stalin, S.; Zhang, Q.; Archer, L.A. Rechargeable lithium metal batteries with an in-built solid-state polymer electrolyte and a high voltage/loading Ni-rich

- layered cathode. *Adv. Mater.* 2020, 32, e1905629.
193. Choudhury, S.; Stalin, S.; Vu, D.; Warren, A.; Deng, Y.; Biswal, P.; Archer, L.A. Solid-state polymer electrolytes for high-performance lithium metal batteries. *Nat. Commun.* 2019, 10, 1–8.
 194. Negi, R.S.; Yusim, Y.; Pan, R.; Ahmed, S.; Volz, K.; Takata, R.; Schmidt, F.; Henss, A.; Elm, M.T. A Dry-Processed Al₂O₃/LiAlO₂ coating for stabilizing the cathode/electrolyte interface in high-Ni NCM-based all-solid-state batteries. *Adv. Mater. Interfaces* 2021, 9, 2101428.
 195. Yersak, T.A.; Hao, F.; Kang, C.; Salvador, J.R.; Zhang, Q.; Malabet, H.J.G.; Cai, M. Consolidation of composite cathodes with NCM and sulfide solid-state electrolytes by hot pressing for all-solid-state Li metal batteries. *J. Solid State Electrochem.* 2022, 26, 709–718.
 196. Xia, Y.; Zheng, J.; Wang, C.; Gu, M. Designing principle for Ni-rich cathode materials with high energy density for practical applications. *Nano Energy* 2018, 49, 434–452.
 197. Li, W.; Song, B.; Manthiram, A. High-voltage positive electrode materials for lithium-ion batteries. *Chem. Soc. Rev.* 2017, 46, 3006–3059.
 198. Li, J.; Li, H.; Stone, W.; Weber, R.; Hy, S.; Dahn, J.R. Synthesis of single crystal LiNi_{0.5}Mn_{0.3}Co_{0.2}O₂ for lithium ion batteries. *J. Electrochem. Soc.* 2017, 164, A3529–A3537.
 199. Yang, C. Superior cycle stability of single crystal nickel-rich layered oxides with micron-scale grain size as cathode material for lithium ion batteries. *Int. J. Electrochem. Sci.* 2020, 15, 5031–5041.
 200. Kim, M.; Zhu, J.; Li, L.; Wang, C.; Chen, G. Understanding reactivities of Ni-rich LiO₂ single-crystal cathode materials. *ACS Appl. Energy Mater.* 2020, 3, 12238–12245.
 201. Pang, P.; Tan, X.; Wang, Z.; Cai, Z.; Nan, J.; Xing, Z.; Li, H. Crack-free single-crystal LiNi_{0.83}Co_{0.10}Mn_{0.07}O₂ as cycling/thermal stable cathode materials for high-voltage lithium-ion batteries. *Electrochim. Acta* 2021, 365, 137380.
 202. Guo, Q.; Huang, J.; Liang, Z.; Potapenko, H.; Zhou, M.; Tang, X.; Zhong, S. The use of a single-crystal nickel-rich layered NCM cathode for excellent cycle performance of lithium-ion batteries. *New J. Chem.* 2021, 45, 3652–3659.
 203. Tian, R.Z.; Wang, Z.X.; Wang, X.Q.; Zhang, H.Z.; Ma, Y.; Song, D.W.; Shi, X.X.; Zhang, L.Q. Preparation and electrochemical investigation of single-crystal LiNi_{0.6}Co_{0.2}Mn_{0.2}O₂ for high-performance lithium-ion batteries. *New J. Chem.* 2022, 46, 4877–4883.
 204. Zhao, Y.; Liu, L.; Cheng, J.; Yang, Z.; Dong, P.; Meng, Q.; Zhang, Y.; Li, Y. Toward high stability single crystal material by structural regulation with high and low temperature mixing sinter. *Ceram. Int.* 2022.
 205. Zhu, H.; Tang, Y.; Wiaderek, K.M.; Borkiewicz, O.J.; Ren, Y.; Zhang, J.; Ren, J.; Fan, L.; Li, C.C.; Li, D.; et al. Spontaneous strain buffer enables superior cycling stability in single-crystal nickel-rich NCM cathode. *Nano Lett.* 2021, 21, 9997–10005.

206. Saleem, A.; Hussain, A.; Ashfaq, M.Z.; Javed, M.S.; Rauf, S.; Hussain, M.M.; Saad, A.; Shen, J.; Majeed, M.K.; Iqbal, R. A well-controlled cracks and gliding-free single-crystal Ni-rich cathode for long-cycle-life lithium-ion batteries. *J. Alloys Compd.* 2022, 924, 166375.
207. Fan, X.; Hu, G.; Zhang, B.; Ou, X.; Zhang, J.; Zhao, W.; Jia, H.; Zou, L.; Li, P.; Yang, Y. Crack-free single-crystalline Ni-rich layered NCM cathode enable superior cycling performance of lithium-ion batteries. *Nano Energy* 2020, 70, 104450.
208. Han, G.M.; Kim, Y.S.; Ryu, H.H.; Sun, Y.K.; Yoon, C.S. Structural stability of single-crystalline ni-rich layered cathode upon delithiation. *ACS Energy Lett.* 2022, 7, 2919–2926.
209. Zhu, J.; Chen, G. Single-crystal based studies for correlating the properties and high-voltage performance of LiO₂ cathodes. *J. Mater. Chem. A* 2019, 7, 5463–5474.
210. Qian, G.; Zhang, Y.; Li, L.; Zhang, R.; Xu, J.; Cheng, Z.; Xie, S.; Wang, H.; Rao, Q.; He, Y.; et al. Single-crystal nickel-rich layered-oxide battery cathode materials: Synthesis, electrochemistry, and intra-granular fracture. *Energy Storage Mater.* 2020, 27, 140–149.
211. Azhari, L.; Meng, Z.; Yang, Z.; Gao, G.; Han, Y.; Wang, Y. Underlying limitations behind impedance rise and capacity fade of single crystalline Ni-rich cathodes synthesized via a molten-salt route. *J. Power Sources* 2022, 545, 231963.
212. Guo, Z.; Jian, Z.; Zhang, S.; Feng, Y.; Kou, W.; Ji, H.; Yang, G. The effect of Ni oxidation state on the crystal structure and electrochemical properties of LiNi_{0.8}Co_{0.1}Mn_{0.1}O₂ cathode material for highly reversible lithium storage. *J. Alloys Compd.* 2021, 882, 160642.
213. Lv, F.; Zhang, Y.; Wu, M.; Gu, Y. A Molten-salt method to synthesize ultrahigh-nickel single-crystalline LiNi_{0.92}Co_{0.06}Mn_{0.02}O₂ with superior electrochemical performance as cathode material for lithium-ion batteries. *Small* 2022, 18, 2201946.
214. Ma, X.; Hou, J.; Vanaphuti, P.; Yao, Z.; Fu, J.; Azhari, L.; Liu, Y.; Wang, Y. Direct upcycling of mixed Ni-lean polycrystals to single-crystal Ni-rich cathode materials. *Chem* 2022, 8, 1944–1955.
215. Ni, L.; Guo, R.; Fang, S.; Chen, J.; Gao, J.; Mei, Y.; Zhang, S.; Deng, W.; Zou, G.; Hou, H.; et al. Crack-free single-crystalline Co-free Ni-rich LiNi_{0.95}Mn_{0.05}O₂ layered cathode. *eScience* 2022, 2, 116–124.
216. Huang, C.; Xia, X.; Chi, Z.; Yang, Z.; Huang, H.; Chen, Z.; Tang, W.; Wu, G.; Chen, H.; Zhang, W. Preparation of single-crystal ternary cathode materials via recycling spent cathodes for high performance lithium-ion batteries. *Nanoscale* 2022, 14, 9724–9735.
217. Liu, L.; Zhang, Y.; Zhao, Y.; Jiang, G.; Gong, R.; Li, Y.; Meng, Q.; Dong, P. Surface growth and intergranular separation of polycrystalline particles for regeneration of stable single-crystal cathode materials. *ACS Appl. Mater. Interfaces* 2022, 14, 29886–29895.

218. Yan, W.; Jia, X.; Yang, S.; Huang, Y.; Yang, Y.; Yuan, G. Synthesis of single crystal $\text{LiNi}_{0.92}\text{Co}_{0.06}\text{Mn}_{0.01}\text{Al}_{0.01}\text{O}_2$ cathode materials with superior electrochemical performance for lithium ion batteries. *J. Electrochem. Soc.* 2020, 167, 120541.
219. Ren, S.; Tian, L.; Shao, Q.; Chen, J. Synthesis of single-crystal $\text{LiNi}_{0.8}\text{Co}_{0.1}\text{Mn}_{0.1}\text{O}_2$ by flux method. *Energy Storage Sci. Technol.* 2020, 9, 1702–1713.
220. Lee, S.H.; Sim, S.J.; Jin, B.S.; Kim, H.S. High performance well-developed single crystal $\text{LiNi}_{0.91}\text{Co}_{0.06}\text{Mn}_{0.03}\text{O}_2$ cathode via LiCl-NaCl flux method. *Mater. Lett.* 2020, 270, 127615.
221. Kimijima, T.; Zettsu, N.; Yubuta, K.; Hirata, K.; Kami, K.; Teshima, K. Molybdate flux growth of idiomorphic $\text{Li}(\text{Ni}_{1/3}\text{Co}_{1/3}\text{Mn}_{1/3})\text{O}_2$ single crystals and characterization of their capabilities as cathode materials for lithium-ion batteries. *J. Mater. Chem. A* 2016, 4, 7289–7296.
222. Li, Y.; He, J.; Luo, L.; Li, X.; Chen, Z.; Zhang, Y.; Deng, L.; Dong, P.; Yang, S.; Wu, K.; et al. Highly dispersed micrometer nickel-rich single-crystal construction: Benefits of supercritical reconstruction during hydrothermal synthesis. *ACS Appl. Energy Mater.* 2022, 5, 6302–6312.
223. Guo, F.; Xie, Y.; Zhang, Y. Low-temperature strategy to synthesize single-crystal $\text{LiNi}_{0.8}\text{Co}_{0.1}\text{Mn}_{0.1}\text{O}_2$ with enhanced cycling performances as cathode material for lithium-ion batteries. *Nano Res.* 2021, 15, 2052–2059.
224. Du, K.; Zhu, F.; Sun, Q.; Hu, G.; Peng, Z.; Cao, Y.; Zhang, Y.; Li, L.; Huang, J.; Zhang, S. $\text{Ni}_{0.6}\text{Co}_{0.2}\text{Mn}_{0.2}(\text{OH})_2$ with dispersed hexagonal slabs enables synthesis of single crystal $\text{LiNi}_{0.6}\text{Co}_{0.2}\text{Mn}_{0.2}\text{O}_2$ with enhanced electrochemical performance for lithium-ion batteries. *J. Alloys Compd.* 2021, 873, 159839.
225. Zhang, D.; Liu, Y.; Feng, L.; Qin, W. Evolution effect of Ti-based modifiers awards improved lithium ion diffusion rate of single crystal nickel-rich cathode. *J. Solid State Chem.* 2022, 306, 122796.
226. Chen, S.; Zhang, X.; Xia, M.; Wei, K.; Zhang, L.; Zhang, X.; Cui, Y.; Shu, J. Issues and challenges of layered lithium nickel cobalt manganese oxides for lithium-ion batteries. *J. Electroanal. Chem.* 2021, 895, 115412.
227. Zhang, Z.; Bai, M.; Fan, X.; Yi, M.; Zhao, Y.; Zhang, J.; Hong, B.; Zhang, Z.; Hu, G.; Lai, Y. A low cost single-crystalline $\text{LiNi}_{0.60}\text{Co}_{0.10}\text{Mn}_{0.30}\text{O}_2$ layered cathode enables remarkable cycling performance of lithium-ion batteries at elevated temperature. *J. Power Sources* 2021, 503, 230028.
228. Zhao, W.; Zou, L.; Zhang, L.; Fan, X.; Zhang, H.; Pagani, F.; Brack, E.; Seidl, L.; Ou, X.; Egorov, K.; et al. Assessing long-term cycling stability of single-crystal versus polycrystalline nickel-rich NCM in pouch cells with 6 mAh cm^{-2} electrodes. *Small* 2022, 18, 2107357.
229. Ryu, H.H.; Lee, S.B.; Sun, Y.K. Promoting grain growth in Ni-rich single-crystal cathodes for high-performance lithium-ion batteries through Ce doping. *J. Solid State Electrochem.* 2022, 26, 2097–

- 2105.
230. Weber, R.; Li, H.; Chen, W.; Kim, C.-Y.; Plucknett, K.; Dahn, J.R. In situ XRD studies during synthesis of single-crystal LiNiO_2 , $\text{LiNi}_{0.975}\text{Mg}_{0.025}\text{O}_2$, and $\text{LiNi}_{0.95}\text{Al}_{0.05}\text{O}_2$ cathode materials. *J. Electrochem. Soc.* 2020, 167, 100501.
231. Liu, A.; Zhang, N.; Stark, J.E.; Arab, P.; Li, H.; Dahn, J.R. Synthesis of Co-free Ni-rich single crystal positive electrode materials for lithium ion batteries: Part I. Two-step lithiation method for Al- or Mg-doped LiNiO_2 . *J. Electrochem. Soc.* 2021, 168, 040531.
232. Liu, A.; Zhang, N.; Stark, J.E.; Arab, P.; Li, H.; Dahn, J.R. Synthesis of Co-free Ni-rich single crystal positive electrode materials for lithium ion batteries: Part II. One-step lithiation method of Mg-doped LiNiO_2 . *J. Electrochem. Soc.* 2021, 168, 050506.
233. Han, Y.; Heng, S.; Wang, Y.; Qu, Q.; Zheng, H. anchoring interfacial nickel cations on single-crystal $\text{LiNi}_{0.8}\text{Co}_{0.1}\text{Mn}_{0.1}\text{O}_2$ cathode surface via controllable electron transfer. *ACS Energy Lett.* 2020, 5, 2421–2433.
234. Guo, J.; Li, W. Synthesis of single-crystal $\text{LiNi}_{0.7}\text{Co}_{0.15}\text{Mn}_{0.15}\text{O}_2$ materials for Li-ion batteries by a sol–gel method. *ACS Appl. Energy Mater.* 2021, 5, 397–406.
235. Ma, X.; Vanaphuti, P.; Fu, J.; Hou, J.; Liu, Y.; Zhang, R.; Bong, S.; Yao, Z.; Yang, Z.; Wang, Y. A universal etching method for synthesizing high-performance single crystal cathode materials. *Nano Energy* 2021, 87, 106194.
236. Malik, M.; Chan, K.H.; Azimi, G. Review on the synthesis of $\text{LiNi}_x\text{Mn}_y\text{Co}_{1-x-y}\text{O}_2$ (NMC) cathodes for lithium-ion batteries. *Mater. Today Energy* 2022, 28, 101066.
237. Zhu, J.; Zheng, J.; Cao, G.; Li, Y.; Zhou, Y.; Deng, S.; Hai, C. Flux-free synthesis of single-crystal $\text{LiNi}_{0.8}\text{Co}_{0.1}\text{Mn}_{0.1}\text{O}_2$ boosts its electrochemical performance in lithium batteries. *J. Power Sources* 2020, 464, 228207.
238. Huang, Z.; Liu, X.; Zheng, Y.; Wang, Q.; Liu, J.; Xu, S. Boosting efficient and low-energy solid phase regeneration for single crystal $\text{LiNi}_{0.6}\text{Co}_{0.2}\text{Mn}_{0.2}\text{O}_2$ via highly selective leaching and its industrial application. *Chem. Eng. J.* 2023, 451, 139039.
239. Gao, D.; Yang, J.; Zhang, D.; Chang, C. An effective strategy to enhance the electrochemical performance of $\text{LiNi}_{0.6}\text{Mn}_{0.2}\text{Co}_{0.2}\text{O}_2$: Optimizing a Li diffusion pathway via magnetic alignment of single-crystal cathode material under an ordinary 0.4-T magnetic field. *Ceram. Int.* 2022, 48, 31598–31605.

Retrieved from <https://encyclopedia.pub/entry/history/show/87792>